

ELECTRONIC SHIELDING BY CLOSED SHELLS
IN
THULIUM COMPOUNDS

Thesis by
John Marlan Poindexter
Lieutenant, United States Navy

In Partial Fulfillment of the Requirements
For the Degree of
Doctor of Philosophy

California Institute of Technology
Pasadena, California
1964

(Submitted May 28, 1964)

PLEASE NOTE:

Figure pages are not original copy.
They tend to "curl". Filmed in the
best possible way.

University Microfilms, Inc.

ACKNOWLEDGEMENTS

The author would like to express his gratitude to Professor R. L. Mössbauer for the privilege of working with him on this experimental project and for guidance in all phases of the research.

Many other people have contributed to the success of these experiments. The author wishes to thank:

Professor R. G. Barnes for his many contributions to the early phase of the calculations and to the development of some of the experimental details.

Professor Felix Boehm for his interest and support of the experimental work.

Dr. E. Kankeleit for many helpful discussions and the design and construction of the transducer drive and associated equipment.

Mr. H. E. Henrikson for the design of the cam drive system and helpful suggestions on the design of other pieces of experimental equipment.

Mr. F. T. Snively for his participation in some of the experimental measurements.

Mr. Vernon Stevens for his help in the reduction of the raw data.

Mr. George Brackett for his aid in many of the technical details.

Dr. J. B. Gruber for making his optical data available prior to publication.

Professor F. H. Spedding for making available the samples of TmES used in this work.

It is a pleasure to acknowledge stimulating discussions with Professors R.J. Elliott, A.J. Freeman, R. Orbach, D.A. Shirley and E. Y. Wong.

The author is participating in the U.S. Navy Junior Line Officer Advanced Scientific Educational Program.

This research was supported in part by the U.S. Atomic Energy Commission.

Mrs. T.O. Anderson deserves all of the credit for the high quality of typing in this thesis.

Finally, the author wishes to thank his wife for her constant cooperation and encouragement.

ABSTRACT

The Mössbauer effect has been used to investigate electronic shielding by closed electron shells in salts of trivalent thulium, by measuring the temperature dependence of the nuclear quadrupole splitting of the 8.42 keV gamma transition in Tm^{169} . The nuclear quadrupole interaction was studied for Tm^{3+} ions in thulium ethyl sulfate, thulium oxide and thulium trifluoride within a temperature range from 9.6°K to 1970°K . The interpretation of the experimental data in terms of the contributions of distorted closed electron shells to the quadrupole interaction yields values for electronic shielding factors. The results lead to amounts of 10% or less for the atomic Sternheimer factor R_Q . The experiments also reveal substantial shielding of the 4f electrons from the crystal electric field, expressed by the shielding factor σ_2 . Values of 250 and 128 are obtained for the ratio $(1-\gamma_\infty)/(1-\sigma_2)$ for thulium ethyl sulfate and thulium oxide respectively, where γ_∞ is the lattice Sternheimer factor.

TABLE OF CONTENTS

<u>PART</u>	<u>TITLE</u>	<u>PAGE</u>
I	INTRODUCTION	1
II	CRYSTAL ELECTRIC FIELD (CEF) INTERACTIONS	7
III	THE NUCLEAR QUADRUPOLE INTERACTION	16
IV	EXPERIMENTAL TECHNIQUE	24
V	EXPERIMENTAL RESULTS AND ANALYSIS	44
VI	ELECTRONIC SHIELDING FACTORS	61
VII	SUMMARY	70
	APPENDIX I	72
	APPENDIX II	80

LIST OF FIGURES

<u>FIGURE</u>	<u>TITLE</u>	<u>PAGE</u>
1	Schematic of atomic and nuclear level splitting	8
2	Partial decay scheme of Er^{169}	25
3	Temperature dependence of quadrupole splitting in TmF_3	28
4	Details of moveable source oven	30
5	Block diagram of experimental apparatus for use with cam drive	34
6	Schematic of programmer	36
7	Proportional counter	38
8	High temperature source oven	40
9	Quadrupole splitting in TmES	42
10	Temperature dependence of quadrupole splitting in TmES	45
11	Temperature dependence of quadrupole splitting in Tm_2O_3	47
12	High temperature quadrupole splitting in TmES and Tm_2O_3	55

LIST OF TABLES

<u>TABLE</u>	<u>TITLE</u>	<u>PAGE</u>
I	Operator equivalents	13-14
II	CEF parameters for TmES	50
III	Observed and calculated CEF levels for TmES in 3H_6 term	51
IV	Energies, wave functions and electric field gradients of CEF levels of 3H_6 in TmES	52
V	Reduced data for Tm^{3+} in TmES and Tm_2O_3	54
VI	Observed and calculated CEF levels and field gradients for Tm_2O_3 in 3H_6 term	59
VII	Theoretical values of Sternheimer shielding factors for rare earth ions	63
VIII	Semi-experimental electronic shielding factors for Tm^{3+}	66

I. INTRODUCTION

The technique of recoilless nuclear resonance absorption of gamma radiation, the so-called Mössbauer effect (1), has been employed in numerous experiments in recent years (2), (3). By binding a radioactive nucleus in a crystal lattice the emitted gamma radiation will, under certain conditions (2), have essentially the natural line width as determined by the Heisenberg uncertainty relation and an energy exactly equal to the excitation energy of the nucleus. If a nucleus of the same isotope which is in its ground state is also bound in a lattice, there is a large probability for nuclear resonance absorption of the gamma radiation. A distinct advantage of this technique is the inherently high energy resolution that is available. For example in the experiments to be described here, the resolution is one part in 10^{11} . Energy resolutions of this order make it possible to study nuclear properties as well as solid state effects in the crystals that are used to bind the nuclei. We make use of the Mössbauer effect here to study the nuclear hyperfine interactions in salts of rare earths, specifically thulium salts.

Measurements of the nuclear quadrupole interaction in salts of the rare earth elements yield information on the quadrupole moments of the relevant nuclear states and on the electric field gradients which

-
- (1) R. L. Mössbauer, *Z. Physik* 151, 124 (1958); *Naturwissenschaften* 45, 538 (1958); *Z. Naturforsch.* 14a, 211 (1959)
 - (2) See for instance H. Frauenfelder, The Mössbauer Effect, (W.A. Benjamin Inc., New York, 1962)
 - (3) The Proceedings of the Third International Conference on the Mössbauer Effect appear in *Rev. Mod. Phys.* 36, 333-504 (1964)

exist in the salts at the nuclear sites. The extraction of the components of the electric field gradient tensor from such measurements is rather straightforward if the values of the nuclear quadrupole moments have been obtained by other methods such as Coulomb excitation techniques. On the other hand the determination of nuclear moments of rare earth nuclei by measurements of the nuclear quadrupole interaction is rather involved since this requires a calculation of the components of the electric field gradient tensor at the nuclear sites. A calculation of the electric field gradients for salts of the rare earths can be performed at present only with limited accuracy. Uncertainties in excess of 30% are typical. It therefore appears that measurements of the nuclear quadrupole interaction in solids of the rare earths are at present of more importance for studies of the sources of the electric field gradients than for determination of nuclear quadrupole moments.

The electric field gradient at the nuclear site of a certain ion originates from a number of different sources. Major sources are distortions of the electronic shells of the ion. These distortions result from the interactions of the electrons of the ion with the crystal electric field (CEF) produced by the surrounding ions in the lattice, provided the arrangement of the surrounding ions reflects a point symmetry lower than cubic. The field gradient at the nuclear site results not only from the distorted partially filled 4f electron shell of the rare earth ion, but also from distorted closed electron shells. These distortions of the closed electron shells of the ion constitute a major source of uncertainty in calculations of the electric field

gradient at the nuclear site. The deviations of the closed shells from spherical symmetry (electric multipole polarization) usually lead to substantial reduction or enhancement (shielding or antishielding) of the electric field gradient at the nuclear site. Sternheimer (4),(5) was first to emphasize the importance of magnetic dipole and electric quadrupole polarizations of closed shells and pioneered in calculating the contributions of closed shell deformations to the nuclear hyperfine interactions.

The nuclear quadrupole interaction depends strongly on the electronic state of the ion. The electronic states which arise when a rare earth ion is incorporated in a crystal lattice are basically caused by the interaction of the CEF and the electrons in the partially filled 4f electron shell, but the splittings of these electronic levels are also strongly influenced by distortions of the closed electron shells (6),(7),(8). In order to account for the modification of the CEF splitting which results from electronic shielding, one has to consider the quadrupole moment as well as higher multipole moments induced in the closed shells.

-
- (4) R.M. Sternheimer, Phys. Rev. 80, 102 (1950); 105, 158 (1957); R.M. Sternheimer and H.M. Foley, *ibid.* 102, 731 (1956); H.M. Foley, R.M. Sternheimer and D. Tyko, *ibid.* 93, 734 (1954)
 - (5) R.M. Sternheimer, Phys. Rev. 84, 244 (1951); 95, 736 (1954)
 - (6) D.T. Edmonds, Phys. Rev. Letters 10, 129 (1963)
 - (7) R.G. Barnes, E. Kankleit, R.L. Mössbauer and J.M. Poindexter, Phys. Rev. Letters 11, 253 (1963)
 - (8) J. Blok and D.A. Shirley (private communication)

Rare earth ions exhibit CEF splittings which are usually very much smaller than similar splittings observed for ions of the iron transition elements. In the iron transition series, the partially filled 3d electron shell is fully exposed to the CEF produced by surrounding ions, resulting in large CEF level splittings. The relatively small CEF level splittings observed for rare earth ions, which typically are of the order of a few hundred cm^{-1} , probably arise because of large shielding effects resulting from the $5s^2 6p^6$ electronic shells which surround the partially filled 4f shell.

Present theoretical predictions of the influence of electronic shielding upon the CEF level splitting of rare earth electronic levels diverge. Burns (9) concluded that electronic shielding in the rare earth ions is of little importance and that the difference between the CEF level splittings in the iron series and those in the rare earth series cannot be attributed to electronic shielding of the 4f electrons from the CEF by outer closed electron shells. In contrast, Lenander and Wong (10), Ray (11) and Watson and Freeman (12) conclude that electronic shielding plays a significant role in rare earth CEF level splittings.

Quantitative estimates of actual shielding effects are hampered by the lack of sufficiently accurate atomic wave functions for rare

(9) G. Burns, Phys. Rev. 128, 2121 (1962)

(10) C.J. Lenander and E.Y. Wong, J. Chem. Phys. 38, 2750 (1963)

(11) D.K. Ray, Proc. Phys. Soc. 82, 47 (1963)

(12) R.E. Watson and A.J. Freeman, Phys. Rev. 133, A1571 (1964)

earth ions. Inadequate knowledge of the contributions of the core electrons is a primary source of uncertainty in our present understanding of hyperfine interactions in rare earth (as well as in other) elements. Direct measurements of the influence of electronic shielding upon the nuclear hyperfine interactions and upon the CEF splittings of electronic levels therefore are highly desirable.

This paper demonstrates the use of the technique of recoilless nuclear resonance absorption of gamma radiation as a means to obtain information on electronic shielding effects in rare earth isotopes. The procedure introduced here consists of combining measurements of the temperature dependent nuclear quadrupole interaction (performed by using the technique of recoilless resonance absorption) with measurements of the CEF level splittings (performed by using optical techniques). Specifically we report on determinations of the relevant electronic shielding factors for trivalent thulium based upon our gamma-absorption measurements of the nuclear quadrupole interaction of Tm^{169} in thulium ethyl sulfate (13) and thulium oxide and on optical measurements of CEF levels by Wong and Richman (14), Gruber and Krupke (15), and Gruber et al. (16).

Tm^{169} appeared to be an isotope particularly suited for studies

-
- (13) A preliminary report of part of this work appeared elsewhere (7).
- (14) E. Y. Wong and I. Richman, J. Chem. Phys. 34, 1182 (1961)
- (15) J. B. Gruber and W. F. Krupke, to be published
- (16) J. B. Gruber, W. F. Krupke and J. M. Poindexter, to be published

of electronic shielding, for the following major reasons:

- (1) The low energy of the 8.4 keV transition used results in a high Debye-Waller factor (recoil-free fraction) even at very high temperatures, thus permitting a measurement of the quadrupole interaction within an unusually wide temperature range.
- (2) The separation of the excited levels belonging to the ground multiplet of thulium ($L = 6; S = 1$) is rather large, with the first excited level (3H_4) some 5600 cm^{-1} above the ground term (3H_6). Thus the existence of the higher levels of the ground multiplet is of minor concern for the interpretation of our data in thulium, in contrast to the situation prevailing in the case of some other rare earth ions.
- (3) The spin of the nuclear ground state ($I = 1/2$) and of the 8.4 keV excited state ($I = 3/2$) is rather low, resulting in a small number of quadrupole hyperfine components of the gamma lines which are easily resolvable.
- (4) The nuclear collective model applies well to Tm^{169} thus permitting a rather reliable semi-theoretical estimate of the nuclear quadrupole moment of the 8.4 keV state.
- (5) The relative abundance of Tm^{169} is 100%.

II. CRYSTAL ELECTRIC FIELD (CEF) INTERACTIONS

A rare earth ion interacts in a salt with the CEF produced by all the ions which surround its position in the lattice. The dominant effect is the interaction of the CEF with the electrons in the partially filled 4f-shell. This interaction is weak compared to the spin-orbit interaction, in contrast with the situation prevailing in the case of iron-transition elements. As a result, the total angular momentum J remains a good quantum number for rare earth ions bound in crystals. The effect of the CEF then essentially is a partial or complete removal of the $2J + 1$ fold spatial degeneracy of the orientation of \underline{J} which exists in a free ion. The actual number of electronic CEF levels depends on the symmetry of the field, while the level spacing depends on the strength of the interactions between the CEF and the 4f electrons. The situation is illustrated in Fig. 1a.

The potential energy describing the interaction between the CEF and a negative charge at position (r, ϑ, φ) within the ion centered at the origin may be represented in good approximation by the following expansion, not including shielding from closed shells:

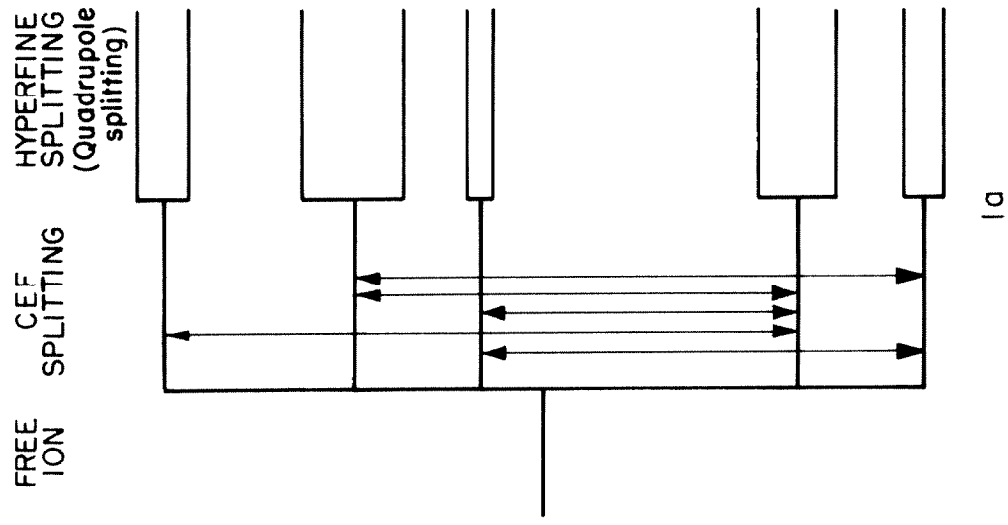
$$-eV(r, \vartheta, \varphi) = \sum_n \sum_{m=-n}^{+n} A_n^m r^n \phi_n^m(\vartheta, \varphi) \quad , \quad (1)$$

if one assumes that there is no overlap between the charge distributions of different ions. In Eq. (1) the A_n^m represent lattice sums over point charges and effective multipole moments in the surrounding ions. The relevant functions ϕ_n^m , which are linear combinations

Fig. 1a: Schematic of the atomic level splitting of a rare earth ion in the CEF. For a nuclear spin $I = 3/2$ the nuclear quadrupole interaction splits each CEF level into a doublet, which is the case illustrated. Typical overall CEF splittings are of the order of 10^{-2} eV, while typical quadrupole hyperfine splittings are of the order of 10^{-6} eV.

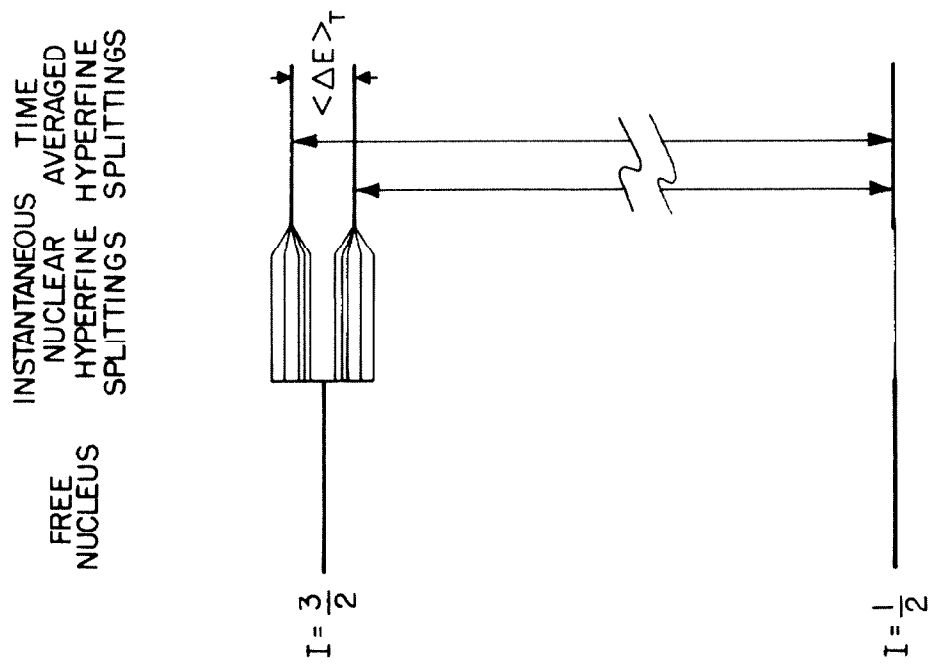
Fig. 1b: Schematic of the nuclear quadrupole splitting of the 8.4 keV transition in Tm^{169} . The temperature dependent level splitting $\langle \Delta E \rangle_T$, which is typically of the order of 10^{-6} eV, is the average of the hyperfine splittings of Fig. 1a, weighted according to their Boltzman factors.

ATOMIC LEVEL SPLITTING



1a

NUCLEAR LEVEL SPLITTING



1b

of spherical harmonics Y_n^m and Y_n^{-m} , are defined as follows (17):

$$\phi_{2n}^0 = (2 \cdot 4 \cdot 6 \dots 2n) P_{2n}(\cos \vartheta)$$

$$\phi_n^{\pm m} = (2)^m (m!) \frac{(n-m)!}{(n+m)!} P_n^m(\cos \vartheta) \cdot \begin{cases} \cos m\varphi \\ \sin m\varphi \end{cases} \quad m > 0$$

where P_n and P_n^m are Legendre polynomials and associated Legendre functions, respectively. In particular, we obtain for $n = 2$:

$$\phi_2^0 = 3 \cos^2 \vartheta - 1 \quad (2a)$$

$$\phi_2^2 = \sin^2 \vartheta \cos 2\varphi \quad (2b)$$

$$\phi_2^{-2} = \sin^2 \vartheta \sin 2\varphi \quad (2c)$$

Specifically, the Hamiltonian describing the interaction between the CEF and the electrons in the partially filled 4f shell of rare earth ions, including the effect of shielding via the closed electron shells of the central ion is given by:

$$H_{\text{CEF}}^{(4f)} = \sum_k \sum_{nm} A_n^m \left[r_k^n + S_n(r_k) \right] \phi_n^m(\vartheta_k, \varphi_k) \quad (3)$$

(17) The normalization of the functions $\phi_n^m(\vartheta, \varphi)$ is arbitrary; the choice adopted here is the one most commonly used

The terms proportional to r_k^n describe the potential energy due to the direct interaction of the CEF with the k-th electron in the 4f-shell while the terms proportional to $S_n(r_k)$ describe the additional potential energy arising from a deformation of the closed electron shells.

The interaction described by the Hamiltonian in Eq.(3) splits the electronic ground state of the free ion, characterized by total angular momentum \underline{J} , into a number of CEF levels. We shall assume in calculating these CEF levels that the angular and radial parts of the free ion wave functions can be factorized and that higher terms with different \underline{J} values can be neglected. Under these circumstances we are dealing with a manifold of states belonging to the same \underline{J} and it is then convenient to replace the angular operators occurring in the Hamiltonian, Eq.(3), by equivalent operators (18). The relevant matrix elements then are of the form

$$H_{m_J m_{J'}} = \sum_{nm} A_n^m \langle r^n \rangle_E \langle \underline{J} \| \vartheta_n \| \underline{J} \rangle \langle \underline{J}, m_J | O_n^m(J_x, J_y, J_z) | \underline{J}, m_{J'} \rangle \quad (4)$$

where $\langle r^n \rangle_E = (1 - \sigma_n) \langle r^n \rangle_{4f} \quad (5)$

-
- (18) K.W.H. Stevens, Proc. Phys. Soc. A65, 209 (1952);
R.J. Elliott and K.W.H. Stevens, Proc. Roy. Soc. A218,
553 (1953); J.P. Elliott, B.R. Judd and W.A. Runciman,
ibid. A240, 509 (1957); R. Orbach, ibid. A264, 458 (1961)

$$\sigma_n = \langle U_{4f} | S_n(r) | U_{4f} \rangle / \langle r^n \rangle_{4f} \quad (6)$$

$$\langle r^n \rangle_{4f} = \langle U_{4f} | r^n | U_{4f} \rangle \quad (7)$$

and $\varphi_n = \alpha, \beta, \gamma \quad \text{for} \quad n = 2, 4, 6$

In these expressions U_{4f} is the radial part of the electronic wave functions for the 4f-shell. The functions $O_n^m(J_x, J_y, J_z)$ are operator equivalents; those relevant for this work are listed in Table I. The expressions $\langle J || \varphi_n || J \rangle$ are reduced matrix elements (19), which for the more general case of intermediate coupling are available for Tm^{3+} in the literature (14)-(17), (20).

It is in principle possible to calculate the parameters A_n^m and $\langle r^n \rangle_E$, but difficult in practice. Difficulties are in the evaluation of the "lattice sums" A_n^m because of a lack of sufficient knowledge of the ionic position coordinates and their temperature dependence as well as of the values of moments in the surrounding ions (21). The evaluation of the radial integrals $\langle r^n \rangle_E$, which are the expectation values of r^n for the 4f shell modified by contributions from closed shells to the electric multipole fields at the 4f electron positions, is hampered by the lack of knowledge of sufficiently accurate atomic

(19) B.R. Judd, Proc. Roy. Soc. A241, 414 (1957)

(20) J.B. Gruber and J.G. Conway, J. Chem. Phys. 32, 1531 (1960)

(21) M.T. Hutchings and D.K. Ray, Proc. Phys. Soc. 81, 663 (1963)

TABLE I. Operator Equivalents

O_2^0	$=$	$3\tilde{\omega}_Z^2 - J(J+1)$
O_2^2	$=$	$1/2 [\tilde{\omega}_+^2 + \tilde{\omega}_-^2]$
O_2^{-2}	$=$	$1/(2i) [\tilde{\omega}_+^2 - \tilde{\omega}_-^2]$
O_4^0	$=$	$[35\tilde{\omega}_Z^4 - [30J(J+1) - 25]\tilde{\omega}_Z^2 - 6J(J+1) + 3J^2(J+1)^2]$
O_4^2	$=$	$1/4 \{ [7\tilde{\omega}_Z^2 - J(J+1) - 5] \cdot (\tilde{\omega}_+^2 + \tilde{\omega}_-^2) + (\tilde{\omega}_+^2 + \tilde{\omega}_-^2) \cdot [7\tilde{\omega}_Z^2 - J(J+1) - 5] \}$
O_4^{-2}	$=$	$1/(4i) \{ [7\tilde{\omega}_Z^2 - J(J+1) - 5] \cdot (\tilde{\omega}_+^2 - \tilde{\omega}_-^2) + (\tilde{\omega}_+^2 - \tilde{\omega}_-^2) \cdot [7\tilde{\omega}_Z^2 - J(J+1) - 5] \}$
O_4^4	$=$	$1/2 [\tilde{\omega}_+^4 + \tilde{\omega}_-^4]$
O_4^{-4}	$=$	$1/(2i) [\tilde{\omega}_+^4 - \tilde{\omega}_-^4]$
O_6^0	$=$	$231\tilde{\omega}_Z^6 - 105 [3J(J+1) - 7]\tilde{\omega}_Z^4 + [105J^2(J+1)^2 - 525J(J+1) + 294]\tilde{\omega}_Z^2$ $- 5J^3(J+1)^3 + 40J^2(J+1)^2 - 60J(J+1)$

(continued)

TABLE I. Operator Equivalents (continued)

$$\begin{aligned}
O_6^2 &= \frac{1}{4} \left\{ [33 \tilde{\omega}_Z^4 - \{ 18J(J+1) + 123 \} \tilde{\omega}_Z^2 + J^2(J+1)^2 + 10J(J+1) + 102] \cdot (J_+^2 + J_-^2) \right. \\
&\quad \left. + (J_+^2 + J_-^2) \cdot [33 \tilde{\omega}_Z^4 - \{ 18J(J+1) + 123 \} \tilde{\omega}_Z^2 + J^2(J+1)^2 + 10J(J+1) + 102] \right\} \\
O_6^{-2} &= \frac{1}{(4i)} \left\{ [33 \tilde{\omega}_Z^4 - \{ 18J(J+1) + 123 \} \tilde{\omega}_Z^2 + J^2(J+1)^2 + 10J(J+1) + 102] \cdot (J_+^2 - J_-^2) \right. \\
&\quad \left. + (J_+^2 - J_-^2) \cdot [33 \tilde{\omega}_Z^4 - \{ 18J(J+1) + 123 \} \tilde{\omega}_Z^2 + J^2(J+1)^2 + 10J(J+1) + 102] \right\} \\
O_6^4 &= \frac{1}{4} \left\{ [11 \tilde{\omega}_Z^2 - J(J+1) - 38] \cdot (\tilde{\omega}_+^4 + \tilde{\omega}_-^4) + (\tilde{\omega}_+^4 + \tilde{\omega}_-^4) \cdot [11 \tilde{\omega}_Z^2 - J(J+1) - 38] \right\} \\
O_6^{-4} &= \frac{1}{(4i)} \left\{ [11 \tilde{\omega}_Z^2 - J(J+1) - 38] \cdot (\tilde{\omega}_+^4 - \tilde{\omega}_-^4) + (\tilde{\omega}_+^4 - \tilde{\omega}_-^4) \cdot [11 \tilde{\omega}_Z^2 - J(J+1) - 38] \right\} \\
O_6^6 &= \frac{1}{2} (\tilde{\omega}_+^6 + \tilde{\omega}_-^6) \\
O_6^{-6} &= \frac{1}{(2i)} (\tilde{\omega}_+^6 - \tilde{\omega}_-^6)
\end{aligned}$$

wave functions for bound rare earth ions. For these reasons it is therefore preferable to introduce the "CEF parameters"

$$C_n^m = A_n^m \langle r^n \rangle_E \quad (8)$$

to be determined by experiment. The point symmetry of the central ion drastically reduces the number of CEF parameters (22). In the case of rare earth ions only the terms with $n = 2, 4, 6$ need to be considered, with the effects of $n = 1, 3, 5$ being negligible in most cases (22).

The wave functions ψ_ν of the ν -th CEF level will be taken as a linear combination of eigenvectors of the total angular momentum \underline{J} ,

$$\psi_\nu = U_{4f}(r) \sum_{m_J} a_\nu^{(m_J)} \psi_J^{m_J} \quad (9)$$

The expansion coefficients $a_\nu^{(m_J)}$ and the energy eigenvalues E_ν follow from the diagonalization of the interaction matrix $H_{m_J, m_J'}$, Eq. (4).

(22) A compilation of the relevant values n and m for various crystal symmetries was given by J. L. Prather, NBS Monograph 19 (1961)

III. THE NUCLEAR QUADRUPOLE INTERACTION

Each of the CEF levels may produce a magnetic field and an electric field gradient at the nuclear site; this results in hyperfine splittings of the electronic levels. A rare earth nucleus thus experiences at a certain time a magnetic field and an electric field gradient which depends on the electronic state that is actually populated at this time. The situation substantially simplifies at elevated temperatures where the spin-lattice relaxation phenomenon produces rapid transition between the different CEF levels. The nucleus under these circumstances experiences a magnetic field and an electric field gradient which in essence result from averaging these fields over all electronic states weighted according to the population numbers. This averaging process, which essentially constitutes a time averaging process, holds only if the significant electron relaxation times are short compared to all other relevant times such as the nuclear lifetimes and the nuclear precession times, a situation prevailing at temperatures above a few degrees Kelvin. In particular, the magnetic hyperfine interaction cancels in the absence of an external magnetic field and all one is left with is the quadrupole hyperfine interaction (23), (24). An example of this situation is illustrated in Fig. 1b for an assembly of nuclei. The quadrupole

(23) R. L. Cohen, U. Hauser and R. L. Mössbauer, Proc. Mössbauer Conf. 2nd, (John Wiley and Sons, N. Y., 1962) p. 172

(24) R. L. Mössbauer, Rev. Mod. Phys. 36, 362 (1964)

interaction is strongly temperature dependent since the overall CEF splitting within the lowest electronic term is only of the order of a few hundred cm^{-1} .

The electric field gradient which interacts with the nuclear quadrupole moment of a rare earth nucleus bound in an ionic crystal has four significant sources:

- 1) One contribution is the direct field gradient produced at the nuclear site by all of the ions surrounding the host ion which contains the nucleus in question. This contribution in the case of rare earth ions is usually negligible in comparison with the contributions from other sources, particularly at low temperatures.
- 2) Another contribution results from the electric field gradient produced at the nuclear site by the electrons in the partially filled 4f-shell of the host ion. This field gradient results from the interaction of the 4f-electrons with the CEF produced by the surrounding ions. This interaction effectively induces electric multipole moments (multipole polarization) in the 4f-shell; the quadrupole part of this polarization contributes to the electric field gradient experienced by the nucleus.
- 3) A distortion is usually also induced by the CEF in the closed electron shells, yielding another contribution to the total field gradient experienced by the nucleus. This contribution is proportional to source (1), with proportionality factor $-\gamma_{\infty}$. The absolute value of the proportionality factor is in the

case of the rare earths usually large in comparison with unity, thereby leading to such an enhanced field gradient (antishielding effect) that it often becomes comparable with the one resulting from source 2). This is the "lattice" Sternheimer effect (25)-(28).

- 4) Another field gradient contribution due to an induced quadrupole moment in the closed electron shells results from the interaction of the closed electron shells with the electrons in the partially filled 4f-shell. This relatively small contribution, which is proportional to source 2), with proportionality factor $-R_Q$, is the "atomic" Sternheimer effect (5), (28).

Collecting the different contributions, we obtain for any component \underline{eq}_{ij} of the electric field gradient tensor

$$\underline{eq}_{ij} = (1-\gamma_\infty) \underline{eq}_{ij}^{(Lat)} + (1-R_Q) \underline{eq}_{ij}^{(4f)} \quad i, j = 1, 2, 3 \quad (10)$$

where γ_∞ and R_Q are the lattice and atomic Sternheimer factors, respectively, as introduced above.

-
- (25) E.G. Wikner and G. Burns, Phys. Letters 2, 225 (1962)
 (26) D.K. Ray, Proc. Phys. Soc. 82, 47 (1963)
 (27) R.M. Sternheimer, Phys. Rev. 132, 1637 (1963)
 (28) A.J. Freeman and R.E. Watson, Phys. Rev. 132, 706 (1963)

In the principle axes system of the electric field gradient tensor the nuclear quadrupole interaction Hamiltonian $H_Q^{(\nu)}$ associated with the (ν) -th CEF level of the ion is given by

$$H_Q^{(\nu)} = \frac{e^2 Q}{4I(2I-1)} \left\{ [(1-R_Q) \langle \nu | q_{zz}^{(4f)} | \nu \rangle + (1-\gamma_\infty) q_{zz}^{(Lat)}] (3\tilde{I}_z^2 - \tilde{I}^2) + [(1-R_Q) \langle \nu | q_{xx}^{(4f)} - q_{yy}^{(4f)} | \nu \rangle + (1-\gamma_\infty) (q_{xx}^{(Lat)} - q_{yy}^{(Lat)})] \frac{1}{2} (\tilde{I}_+^2 + \tilde{I}_-^2) \right\} \quad (11)$$

where $\tilde{I}_z, \tilde{I}_\pm$ are the usual nuclear spin operators and Q is the nuclear quadrupole moment. The quantities $q_{ii}^{(Lat)}$ and $\langle \nu | q_{ii}^{(4f)} | \nu \rangle$ determine the direct contributions to the electric field gradient at the nuclear site produced by the surrounding ions in the lattice and by the 4f-electrons of the host ion, respectively. They are defined by

$$eq_{ii}^{(Lat)} = [\partial^2 V(r, \vartheta, \varphi) / \partial x_i \partial x_i]_{r=0}, \quad (12)$$

where $V(r, \vartheta, \varphi)$ is defined in Eq.(1), and

$$\langle \nu | q_{ii}^{(4f)} | \nu \rangle = \langle \nu | \sum_k^{4f\text{-electrons}} [\partial^2 \left(\frac{-1}{|\underline{r}_k - \underline{r}|} \right) / \partial x_i \partial x_i]_{r=0} | \nu \rangle \quad (13)$$

where the wave function $|\nu\rangle$ of the ν -th CEF level is of the form given by Eq.(9).

Explicitly we obtain for the lattice contribution from Eqs.(1), (2), (12)

$$e^2 q_{zz}^{(Lat)} = -4A_2^0 \quad ; \quad e^2 (q_{xx}^{(Lat)} - q_{yy}^{(Lat)}) = -4A_2^2 \quad (14)$$

Expressing the contributions from the 4f -electrons within a manifold of states of constant \underline{J} in terms of operator equivalents, we obtain from Eq. (13)

$$\langle \nu | q_{zz}^{(4f)} | \nu \rangle = -\langle J \| \alpha \| J \rangle \langle r^{-3} \rangle_{4f} \langle \nu | 3J_z^2 - J^2 | \nu \rangle \quad (15a)$$

$$\langle \nu | q_{xx}^{(4f)} - q_{yy}^{(4f)} | \nu \rangle = -(3/2) \langle J \| \alpha \| J \rangle \langle r^{-3} \rangle_{4f} \langle \nu | J_+^2 - J_-^2 | \nu \rangle \quad (15b)$$

where $\langle r^{-3} \rangle_{4f}$ is defined by Eq. (7).

Usually one observes only an average field gradient from the 4f-electrons, which is a field gradient from the individual CEF levels weighted according to their Boltzman factors, as discussed above. If we consider only those electronic states which belong to the lowest manifold spanned by the state vector \underline{J} , then the average direct contribution from the 4f-electrons to the electric field gradient acting on the nucleus at temperature T is given by (29)

$$\langle q_{ii}^{(4f)} \rangle_T = \frac{\sum_{\nu=1}^{2J+1} \langle \nu | q_{ii}^{(4f)} | \nu \rangle \cdot \exp(-E_\nu / kT)}{\sum_{\nu=1}^{2J+1} \exp(-E_\nu / kT)} \quad (16)$$

The diagonal component of the averaged total electric field gradient tensor is according to Eqs. (10) and (16) given by

(29) A more general description including effects of higher J states is given in the Appendix I

$$\langle q_{ii} \rangle_T = (1 - \gamma_\infty) q_{ii}^{(\text{Lat})} + (1 - R_Q) \langle q_{ii}^{(4f)} \rangle_T \quad (17)$$

where we have neglected any temperature dependence of the lattice contribution $q_{ii}^{(\text{Lat})}$.

The total Hamiltonian describing the average quadrupole interaction at temperature T may now according to Eqs.(11) and (17) be written as

$$H_Q(T) = \frac{e^2 Q}{4I(2I-1)} \left[\langle q_{zz} \rangle_T (3\tilde{I}_z^2 - I^2) + \langle q_{xx} - q_{yy} \rangle_T \frac{1}{2} (\tilde{I}_+^2 + \tilde{I}_-^2) \right] \quad (18)$$

We shall now apply the preceding formalism to the particular case of Tm^{169} . The twofold degeneracy of the nuclear ground state of Tm^{169} ($I = 1/2$) is not removed by the Hamiltonian, Eq.(18); the 8.4 keV excited state ($I = 3/2$), on the other hand, is split by the nuclear quadrupole interaction into two states. Their energy separation $\langle \Delta E \rangle_T$ which follows from the diagonalization of the Hamiltonian $H_Q(T)$ is given by

$$\langle \Delta E \rangle_T = (e^2 Q/2) \left[\langle q_{zz} \rangle_T^2 + \frac{1}{3} \langle q_{xx} - q_{yy} \rangle_T^2 \right]^{\frac{1}{2}} \quad (19)$$

This expression may be written in more detail, by using Eqs.(5), (8), (14), (15), (17):

$$\begin{aligned} \langle \Delta E \rangle_T = (e^2 Q / 2) \left\{ \left[\langle J \parallel \alpha \parallel J \rangle \langle r^{-3} \rangle_Q \langle 3J_z^2 - J^2 \rangle_T + \frac{4C_2^0}{e^2 \langle r^2 \rangle_E} (1 - \gamma_\infty) \right]^2 \right. \\ \left. + \frac{1}{3} \left[\frac{3}{2} \langle J \parallel \alpha \parallel J \rangle \langle r^{-3} \rangle_Q \langle J_+^2 + J_-^2 \rangle_T + \frac{4C_2^2}{e^2 \langle r^2 \rangle_E} (1 - \gamma_\infty) \right]^2 \right\}^{\frac{1}{2}} \end{aligned} \quad (20)$$

where $\langle 3J_z^2 - J^2 \rangle_T$ and $\langle J_+^2 + J_-^2 \rangle_T$ are thermal averages defined as those given by Eq.(16), while the parameter $\langle r^{-3} \rangle_Q$ is defined by

$$\langle r^{-3} \rangle_Q = (1 - R_Q) \langle r^{-3} \rangle_{4f} \quad (21)$$

It is just this splitting $\langle \Delta E \rangle_T$ that is measured as a separation of gamma lines in recoilless resonance absorption experiments.

Several additional hyperfine interaction mechanisms which contribute to the net nuclear quadrupole coupling of a rare earth ion have been neglected in our calculations. These additional contributions arise in second-order perturbation theory with the principal effects coming from the magnetic hyperfine interaction itself (30) (the so-called pseudo-quadrupole coupling) and from the quadrupole interaction with states of higher J admixed into the ground state multiplet by the CEF. We have made calculations of these contributions for the compounds covered in this paper and they amount to less than 1% of the total quadrupole interaction energy.

In order to compare experimental results with theory within the framework of the CEF model it is convenient to replace in the theo-

(30) R.J. Elliott, Proc. Phys. Soc. B70, 119 (1957)

retical expression for the quadrupole splitting $\langle \Delta E \rangle_T$ all quantities involving electronic radial integrals (the theoretical determinations of which is presently somewhat uncertain) as well as the nuclear quadrupole moment by experimentally observable parameters. For this purpose we introduce the dimensionless parameters

$$\rho_1 = e^2 Q \langle r^{-3} \rangle_Q \langle J \| \alpha \| J \rangle / C_2^0 \quad (22a)$$

$$\rho_2 = Q(1 - \gamma_\infty) / \langle r^2 \rangle_E \quad (22b)$$

Expressed in terms of these parameters the quadrupole splitting in Tm^{169} reduces to

$$\begin{aligned} \langle \Delta E \rangle_T = \frac{1}{2} \left\{ \left[C_2^0 \rho_1 \langle 3\tilde{J}_z^2 - \tilde{J}^2 \rangle_T + 4C_2^0 \rho_2 \right]^2 + \right. \\ \left. + \frac{1}{3} \left[(3/2) C_2^0 \rho_1 \langle \tilde{J}_+^2 + \tilde{J}_-^2 \rangle_T + 4C_2^2 \rho_2 \right]^2 \right\}^{\frac{1}{2}} \end{aligned} \quad (23)$$

The temperature averages $\langle 3\tilde{J}_z^2 - \tilde{J}^2 \rangle_T$ and $\langle \tilde{J}_+^2 + \tilde{J}_-^2 \rangle_T$ within the framework of the CEF model depend only on the experimentally observable CEF parameters C_n^{m1} .

IV EXPERIMENTAL TECHNIQUE

The nuclear quadrupole interaction was measured by using the technique of the recoilless nuclear resonance absorption of gamma radiation (2). The partial decay scheme of Er^{169} is shown in Fig. 2. Measurements of the gamma resonance absorption were performed as a function of the relative velocity between sources and absorbers. The measurements involved sources of erbium trifluoride (ErF_3) and erbium oxide (Er_2O_3) and absorbers of thulium ethyl sulfate ($\text{Tm}(\text{C}_2\text{H}_5\text{SO}_4)_3 \cdot 9\text{H}_2\text{O}$, abbreviated to TmES) and thulium oxide (Tm_2O_3).

Anhydrous ErF_3 provides an excellent source for experiments utilizing the 8.4 keV line of Tm^{169} . The crystal structure of the heavy rare-earth trifluorides has been investigated by Zalkin and Templeton (31). At temperatures below about $900 - 1000^\circ\text{C}$ the stable phase is orthorhombic, space group D_{2h}^{16} -Pnma, having four formula units per unit cell. The rare earth ions are crystallographically equivalent, having the point symmetry m . Thus, although the electric field gradient tensor \tilde{eq}_{ij} is not axially symmetric, all erbium (or thulium) nuclei experience the same \tilde{eq}_{ij} . Therefore, the quadrupole splitting of the recoilless absorption line given by Eq. (23), may be expected to pass through zero or at least through a minimum at a specific temperature (550°K in this case). The advantages of a single-line source are thereby obtained. The line width obtained this way with sources of ErF_3 is less than with sources of

(31) A. Zalkin and D.H. Templeton, J. Am. Chem. Soc. 75, 2453 (1953)

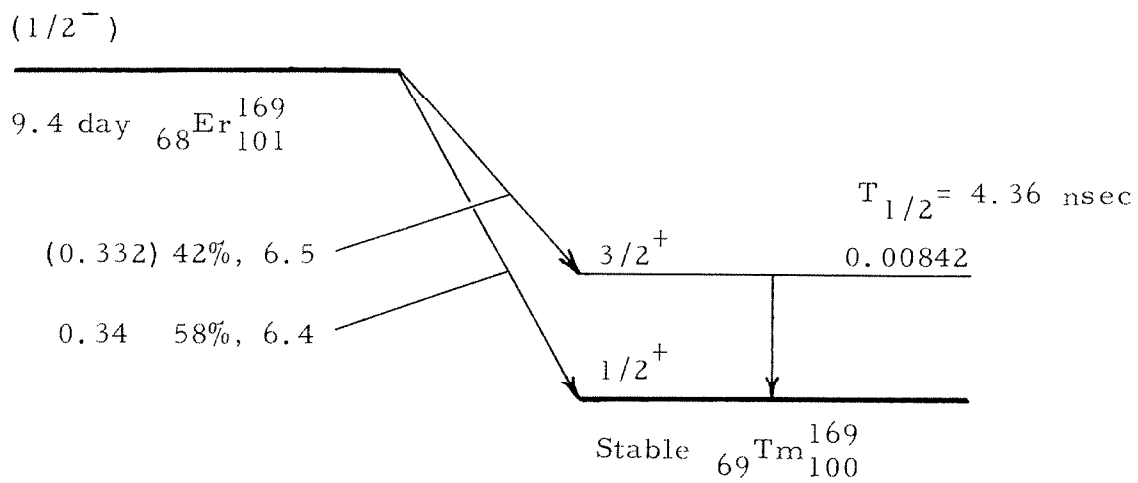


Fig. 2: Partial decay scheme of Er^{169} .

Er_2O_3 where the presence of non-equivalent erbium sites complicates the situation (23), (24). At the same time, with reasonable precautions, the ErF_3 can be maintained at the critical temperature for periods of several weeks without decomposition or reaction. This chemical stability does not exist with most other erbium salts in which the erbium ions are also crystallographically equivalent (e. g., the sulfate, nitrate, chloride).

Anhydrous ErF_3 was prepared from erbium metal or erbium oxide by a "wet" process. The metal or oxide was first dissolved in a small quantity of nitric or hydrochloric acid in polyethylene centrifuge tube. A few ml of aqueous hydrofluoric acid were then added and the mixture heated at approximately 100°C in a water bath for 30 minutes. The somewhat gelatinous ErF_3 precipitate was then centrifuged down, the excess solution decanted off, the precipitate washed with distilled water, centrifuged three to five times and dried in air at roughly 100°C . Air drying yields a hydrated ErF_3 of unknown composition. To remove the water of hydration, the dry contents of the centrifuge tube bottom were transferred to a small tantalum boat and annealed in an evacuated fused quartz tube. Experience showed that the hydrated ErF_3 could be converted directly into a mixture of the several forms of oxyfluoride (32) if the annealing temperature was raised too rapidly. The procedure finally adopted was to hold the hydrate at room temperature at about 10^{-5} torr for at least 12 hours in order to pump off most of the water. The temperature was

(32) W. H. Zachariasen, Acta Cryst. 4, 231 (1951)

then raised slowly (in 6 hours) to 150°C , thus removing virtually all of the water. Finally, the temperature was raised to 850°C in another 6 hours and then reduced back to room temperature within 2 hours. This procedure yielded consistently good clean x-ray powder patterns of the orthorhombic phase without a trace of the hexagonal phase appearing (31). ErF_3 prepared in this manner appears to remain stable at room temperature over an indefinite period of time. At elevated temperatures care must be exercised to avoid reaction with oxygen or water vapor. Sources of ErF_3 were prepared in the above manner from Er_2O_3 (usually enriched in Er^{168}) or from erbium metal after irradiation in the Materials Testing Reactor, Arco, Idaho. Alternatively, the ErF_3 was prepared first and then irradiated. Identical spectra were obtained by the two methods.

Absorbers of TmF_3 were used in order to experimentally determine the critical temperature at which the narrowest possible emission line is obtained with sources of ErF_3 . Figure 3 shows the temperature dependence of the quadrupole splitting in TmF_3 . The source was mounted in a small evacuated oven shown in Fig. 4. The absorber was maintained in a helium atmosphere within an oven equipped with beryllium windows.

It is interesting to note that the same minimum line width (1.8 cm/sec) was obtained in both the trifluoride-trifluoride and trifluoride-ethylsulfate experiments. This strongly suggests that the quadrupole splitting of the trifluoride line does indeed pass very near to zero at 550°K (24). This minimum observed line width of 1.8 cm/sec may be compared with the theoretically predicted line

Fig. 3: Temperature dependence of the quadrupole splitting of the 8.4 keV gamma line of Tm^{169} using an ErF_3 source and a TmF_3 absorber. Source and absorber were maintained at the same temperature.

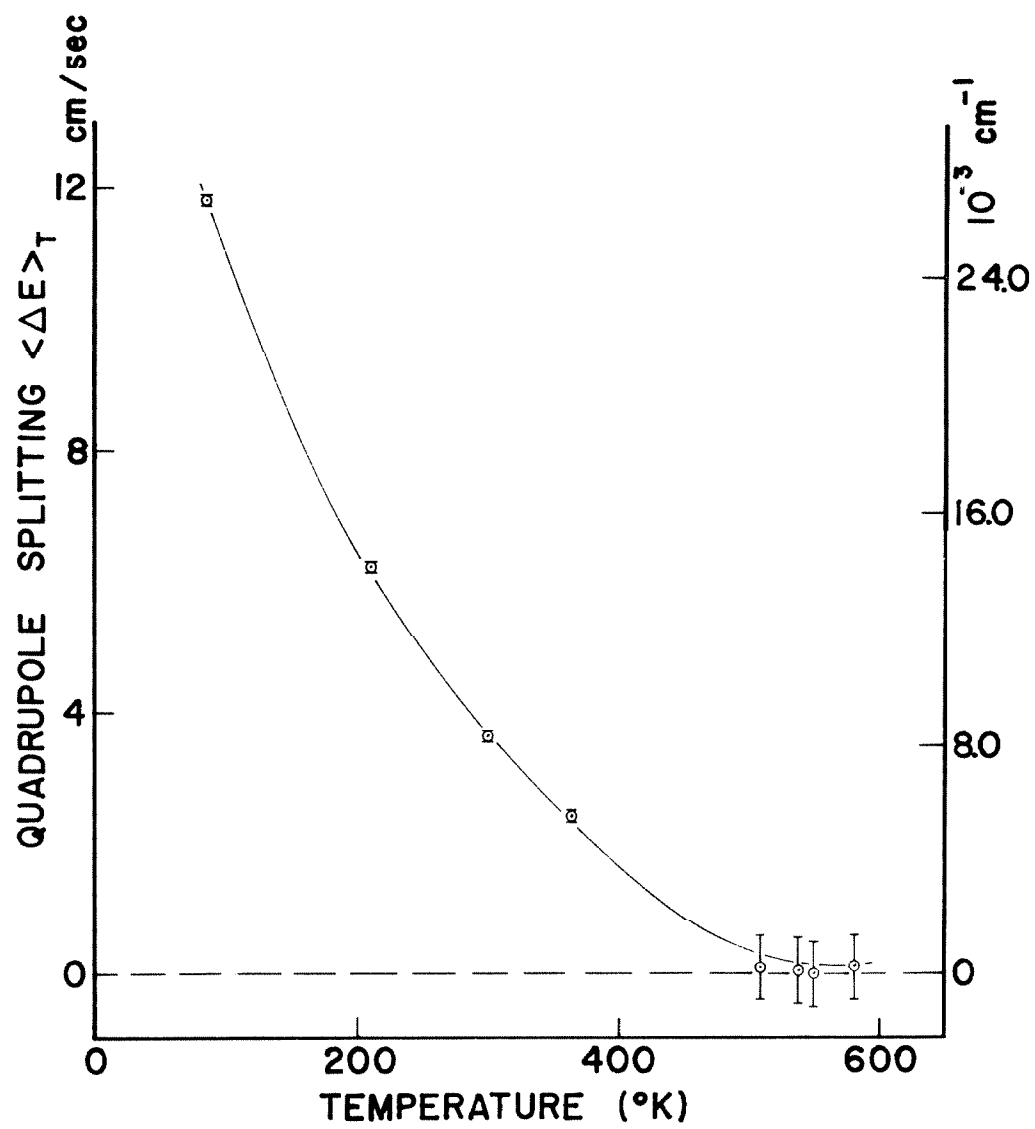


FIG. 3.

Fig. 4: Details of moveable source oven. The entire oven (weight 0.2 kg) was moved relative to the absorber by the cam drive. The main body of the oven was made of stainless steel. A similar oven made of aluminum was used with the transducer drive. The heating element was fabricated from nichrome strips, $1/16 \times 0.005$ in. For a source temperature of 550°K the power input was 30 W.

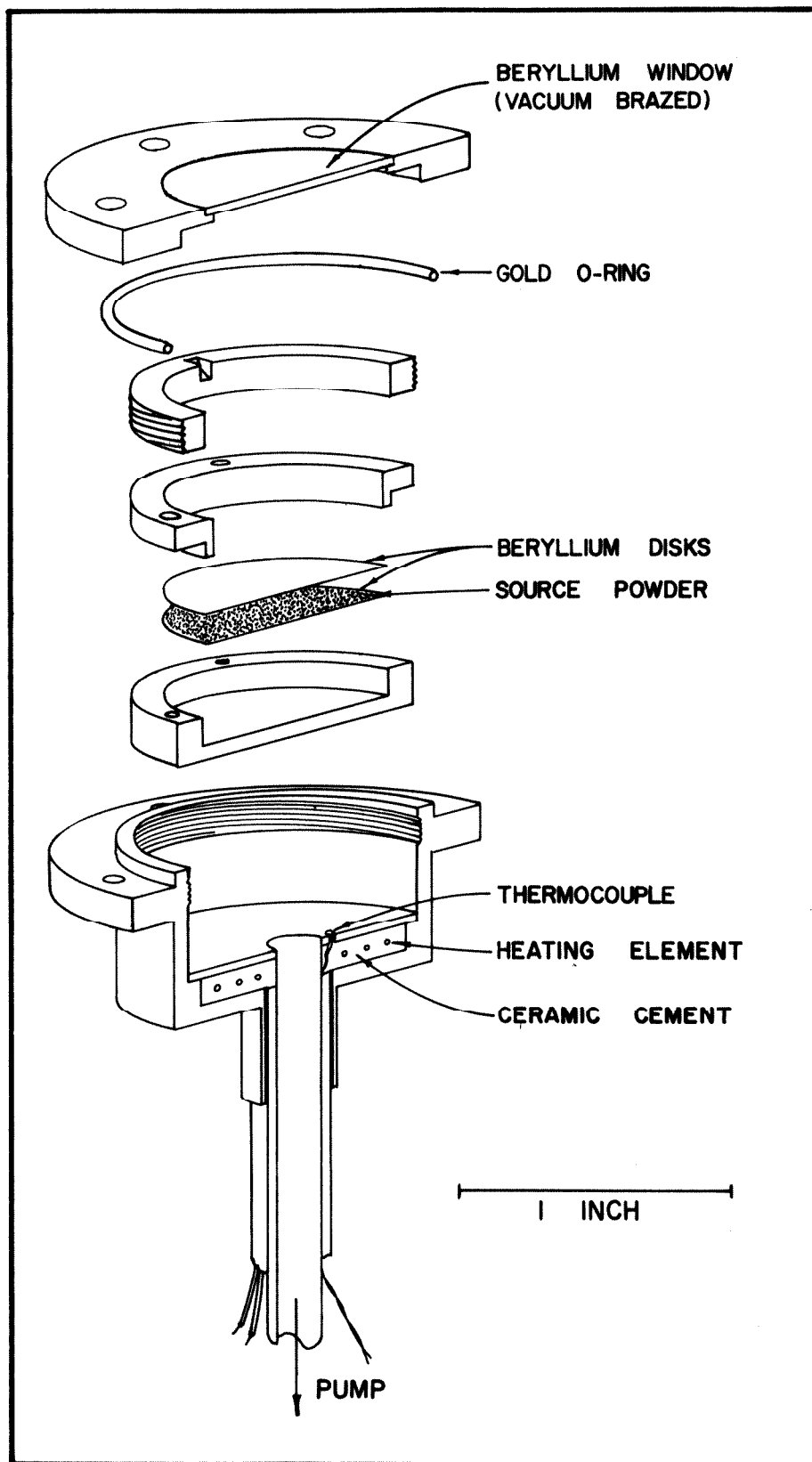


FIG. 4.

width. In a transmission-vs-velocity measurement since an emission line of width Γ is moved over an absorption line of width Γ , one expects a minimum line width of 2Γ . In the case at hand this is (in velocity units)

$$2\Gamma c/E_{\gamma} = 2\hbar c/\tau E_{\gamma} = 0.74 \text{ cm/sec}$$

based on the lifetime (33), $\tau = 6.28 \cdot 10^{-9}$ sec, and energy, $E_{\gamma} = 8.42$ keV, of the first excited state of Tm^{169} . However for an absorber of finite thickness this width increases by a correction factor which is 1.47 in our case for an absorber of 5 mg/cm^2 of thulium and a total conversion coefficient of 325 from Kankeleit et al. (34). Thus the predicted line width is 1.09 cm/sec which must be compared with the minimum observed line width of 1.8 cm/sec . The observed line width is 1.6 times broader than expected. The origin of this line broadening is uncertain.

Absorbers of TmES were prepared by crushing single crystals. Absorbers of Tm_2O_3 and sources of (enriched) Er_2O_3 were prepared from commercially available material. Absorbers of all materials to be used below room temperature were prepared by mixing the powdered samples with a soft wax and pressing the mixture into thin disks between mylar films. Absorbers and sources of all materials

(33) R. E. McAdams, G. W. Eakins, E. N. Hatch, Phys. Letters 6, 219 (1963)

(34) E. Kankeleit, F. Boehm, R. Hager, Phys. Rev. in press

to be used above room temperature were prepared by settling the powdered samples from a slurry of dry acetone onto 1/2 mm thick beryllium windows.

The relative velocities required for Doppler-shifting the gamma lines were produced by using both cam drives (35) (providing constant velocities) and transducer drives (36) (providing constant acceleration). A block diagram showing the experimental apparatus for use with the cam drive is shown in Fig. 5. The experimental arrangement used with the transducer drive is given in Ref. (36). Proportional counters filled with one atmosphere of a mixture of 90% argon and 10% methane (by volume) and equipped with 1/2 mm thick beryllium windows were used as detectors, see Fig. 7.

A cryostat specifically designed for recoilless resonance absorption experiments with low energy gamma radiation was used for the measurements (37). The sample temperatures in the range from 10⁰K up to 300⁰ K were attained by either controlled heating of the cooled sample holder, by pumping on liquified gases, or by using exchange gas cooling. The sample disks were clamped between thin beryllium disks soldered to the cryostat sample holder in order to ensure good temperature uniformity and stability. Temperature measurements were made using carbon resistors and thermocouples. The oven used for heating sources to 2000⁰ K is shown in Fig. 8.

Some typical Mössbauer spectra for Tm¹⁶⁹ are shown in Fig. 9.

-
- (35) R. L. Mössbauer, Proc. Mössbauer Conf. 2nd, (John Wiley and Sons, New York, 1962), p. 38
- (36) E. Kankeleit, Rev. Sci. Instr. 35, 194 (1964)
- (37) F. T. Snively, to be published

Fig. 5: Block diagram of experimental apparatus for use with the cam drive. A detailed schematic of the programmer is presented in Fig. 6. All other electronic equipment shown is commercially available. The cam drive has been described elsewhere (35). The recoilless resonance absorption measurements were performed by first moving the source at a normalizing speed (12 cm/sec), then at a measuring speed (v), and finally at the normalizing speed. The three runs were of about 5 min each. The counting rates, C , during the two normalizing runs were averaged and combined with the results of the measuring speed to yield the amount of absorption, $A(v)$.

$$A(\pm v) = [C(\pm 12)_{\text{AVE}} - C(\pm v)] / C(\pm 12)_{\text{AVE}}$$

This sequence of events was repeated until the counting statistics were satisfactory. The information at the end of each run was printed out on a typewriter for monitoring purposes and punched out on paper tape for processing by an electronic computer. The entire process was automatic except for changing from one measuring speed to another.

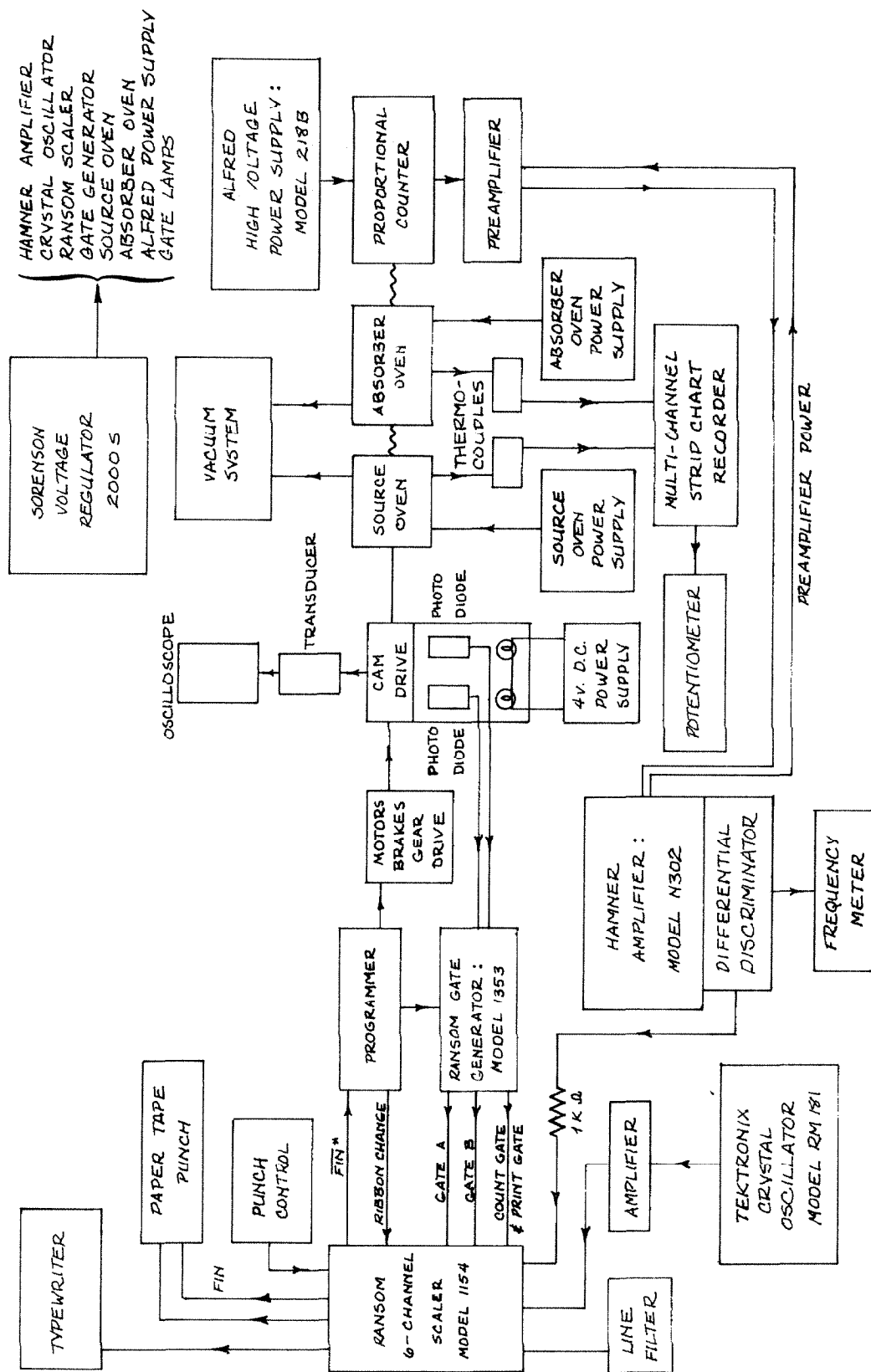


FIG. 5.

Fig. 6: Schematic of programmer for use with cam drive. This programmer controlled the changes from the normalizing speed to the measuring speeds and initiated the counting and print-out cycles of the scaler, see Fig. 5.

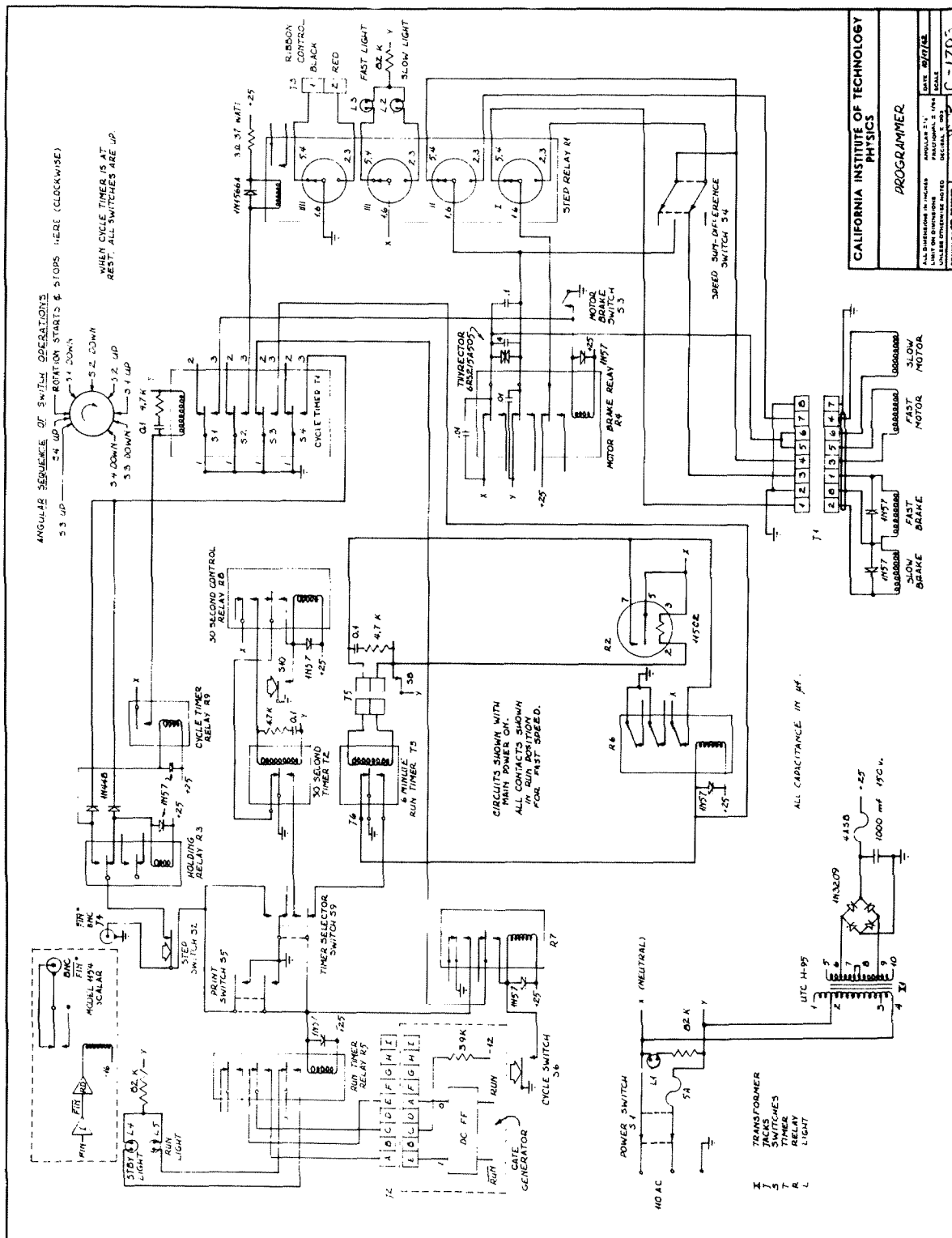


FIG. 6.

Fig.7: Proportional counter. The anode of the counter is a 3 mil stainless steel wire kept under light tension by a spring in the end fitting. The beryllium window is 0.5 mm thick. This counter was operated at about 2500 V with 1 atm of 90% argon and 10% methane, by volume. Under these conditions the resolution at 8.42 keV was about 17%.

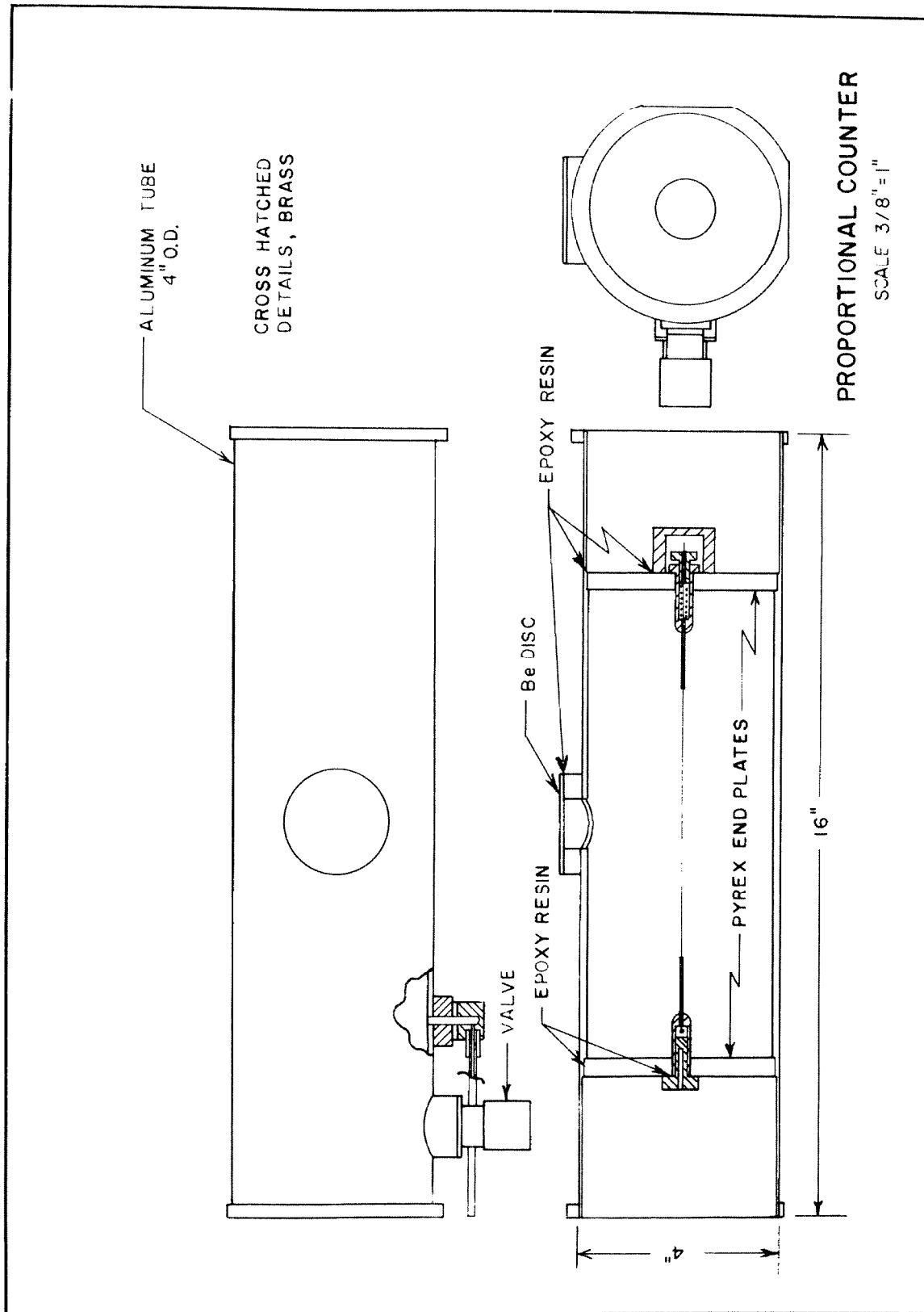


FIG. 7.

Fig. 8: High temperature, resistance heating, source oven. The heating coil was fabricated from two pieces of 56 mil tungsten wire 15 in long. These two pieces were connected in parallel and the source container was suspended from the midpoint of each piece. For a source temperature of 1970°K the power input was 4.8 kW. A vacuum of 10^{-4} torr was maintained in the oven. The thermocouple made of tungsten vs. tungsten - 26% rhenium is reliable to 3100°K .

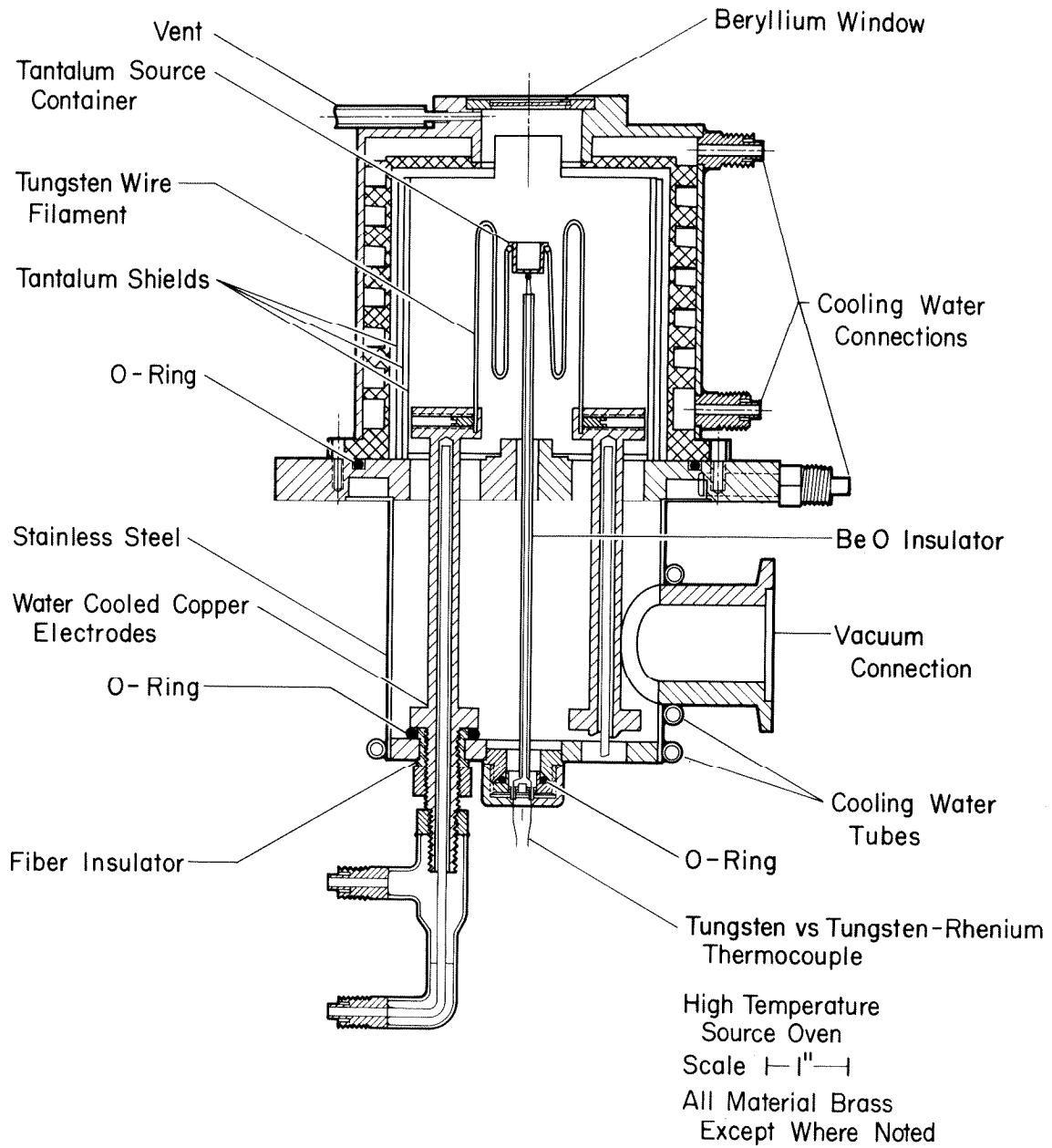


FIG. 8.

Fig. 9: Quadrupole splitting of the 8.4 keV level of Tm^{169} in an absorber of thulium ethyl sulfate (5 mg/cm^2 of thulium). A "single line" source of Er^{169} in ErF_3 was used at the critical temperature $T = 550^\circ \text{K}$ throughout curves a-d. The spectra a, b and c, d were obtained by using a cam drive and a transducer drive, respectively.

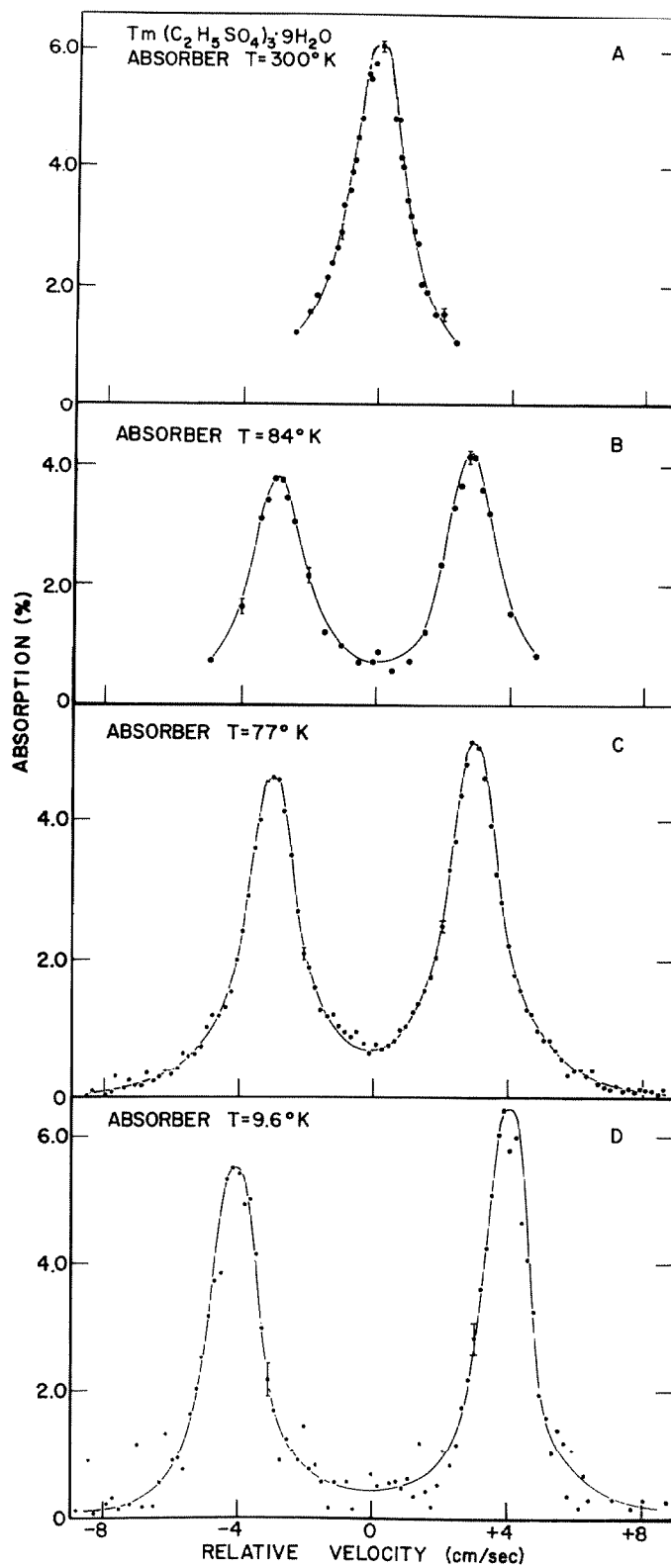


FIG. 9.

V. EXPERIMENTAL RESULTS AND ANALYSIS

The nuclear quadrupole interactions measured as a function of temperature in the compounds TmES and Tm₂O₃ are given in Figs. 10 and 11, respectively. Details of the figures are explained below. The reduction of our experimental results is carried out in two substantially different ways:

Method 1: We combine our nuclear quadrupole splittings obtained from gamma resonance absorption measurements with optically determined CEF levels and obtain two quantities $\rho_1 C_2^0 [(C_2^0)^2 + \frac{1}{3} (C_2^2)^2]^{\frac{1}{2}}$ and $\rho_2 [(C_2^0)^2 + \frac{1}{3} (C_2^2)^2]^{\frac{1}{2}}$ which depend directly on the electronic shielding factors, compare Eqs.(5), (21), (22). This method emphasizes the low temperature data, which have the smallest relative errors.

Method 2: The same two quantities may be obtained without the necessity of referring to any optical determination of CEF levels, merely by using gamma resonance measurements obtained at elevated temperatures. This method is useful in those cases where measurements can be performed at temperatures which are large compared to the overall CEF level splitting, but small compared to the spin-orbit splitting. This is the case in both TmES and Tm₂O₃.

1. Thulium Ethyl Sulfate (TmES)

All rare earth lattice sites in TmES are occupied by Tm³⁺ ions with point group symmetry C_{3h}. By choosing the proper coordinate system (22) the relevant CEF parameters as defined by Eq.(8) are limited to C₂⁰, C₄⁰, C₆⁰ and C₆⁶ for this symmetry. This leads to an

Fig. 10: Temperature dependence of the nuclear quadrupole interaction of Tm^{169} in absorbers of thulium ethyl sulfate (TmES). Sources of ErF_3 ($T = 550^\circ\text{K}$; single line) were used. Curve A is the best two-parameter-fit (parameters ρ_1 and ρ_2) to the experimental data. Curve B is the best one-parameter-fit (parameter ρ_1) to the experimental data, thus disregarding the lattice contribution to the electronic shielding (i. e. $\sigma_2 = \gamma_\infty = 0$). The CEF parameters in set 3 of Table II were used in both curves A and B. Observe that $\langle \Delta E \rangle_{T \rightarrow \infty} \rightarrow 0$ for curve B.

The difference between curves A and B shows the large contribution of the lattice part $(1 - \gamma_\infty) q_{ii}^{(\text{Lat})}$ to the electric field gradient at the nucleus. Curve B illustrates in particular, that it is not possible to obtain a good fit to the experimental data by merely adjusting the theoretical value of either Q or R_Q .

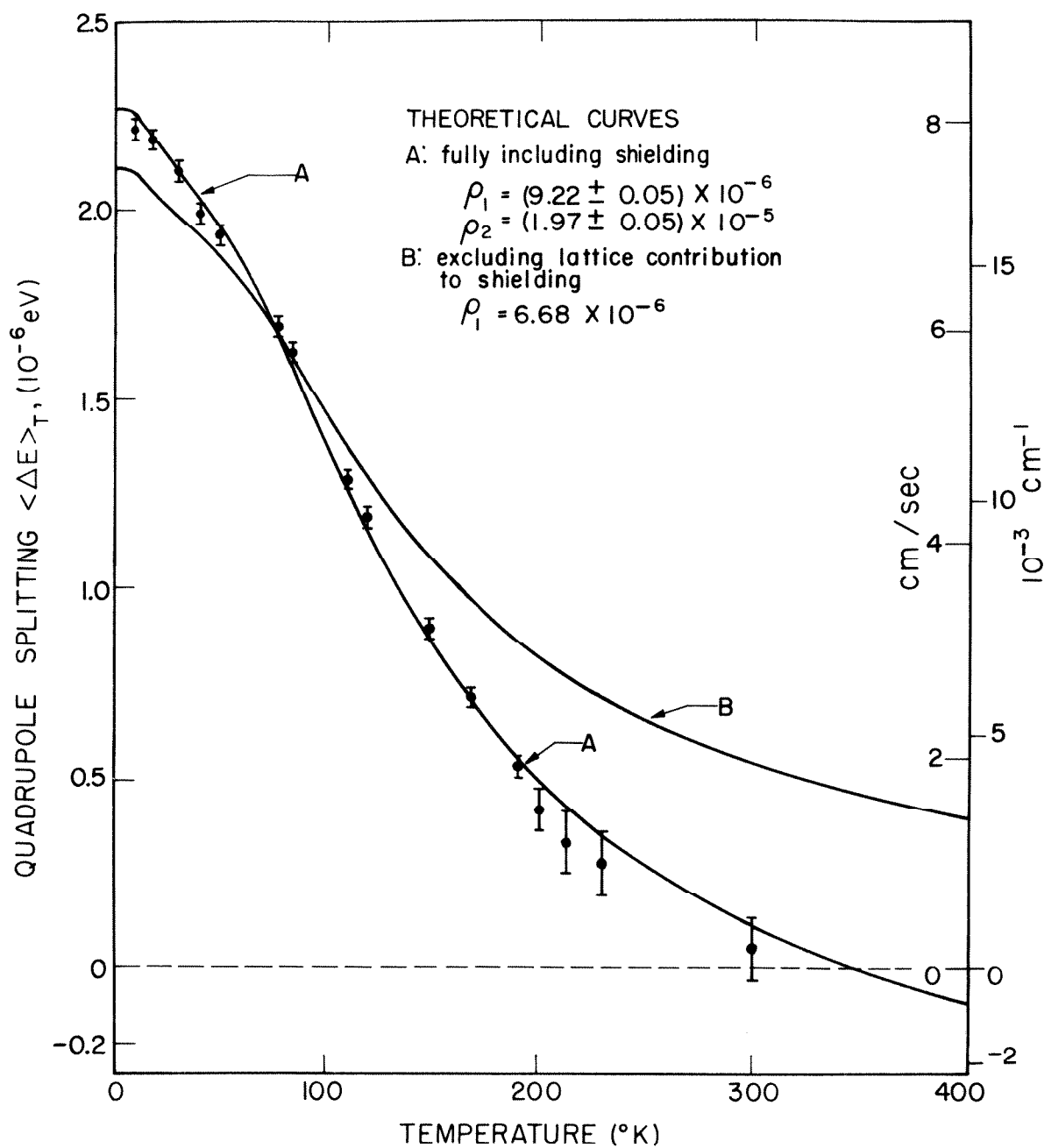


FIG. 10.

Fig. 11: Temperature dependence of the nuclear quadrupole interaction of Tm^{169} in Tm_2O_3 . Sources of ErF_3 ($T = 550^\circ\text{K}$; single line) and absorbers of Tm_2O_3 (5 mg/cm^2 of thulium) were used for temperatures of the absorber in the range $11^\circ\text{K} < T < 700^\circ\text{K}$. Absorbers of TmES ($T = 300^\circ\text{K}$; single line; 5 mg/cm^2 of thulium) and sources of Er_2O_3 were used for temperatures of the source in the range $T > 700^\circ\text{K}$. Curve A is the best two-parameter-fit (parameters ρ_1 and ρ_2) to the experimental data, using the CEF parameters of Table VI. The insert shows a typical spectrum. The importance of the lattice contribution $(1-\gamma_\infty) q_{ii}^{(\text{Lat})}$ to the total field gradient $(1-\gamma_\infty) q_{ii}^{(\text{Lat})} + (1-R_Q) q_{ii}^{(4f)}$ at the nuclear sites is strikingly demonstrated by the fact, that the quadrupole splitting $\langle \Delta E \rangle_T$ does not approach zero in the high temperature limit, but rather goes through a minimum and then increases again, with $\langle q_{ii} \rangle_{T \rightarrow \infty} \rightarrow (1-\gamma_\infty) q_{ii}^{(\text{Lat})}$.

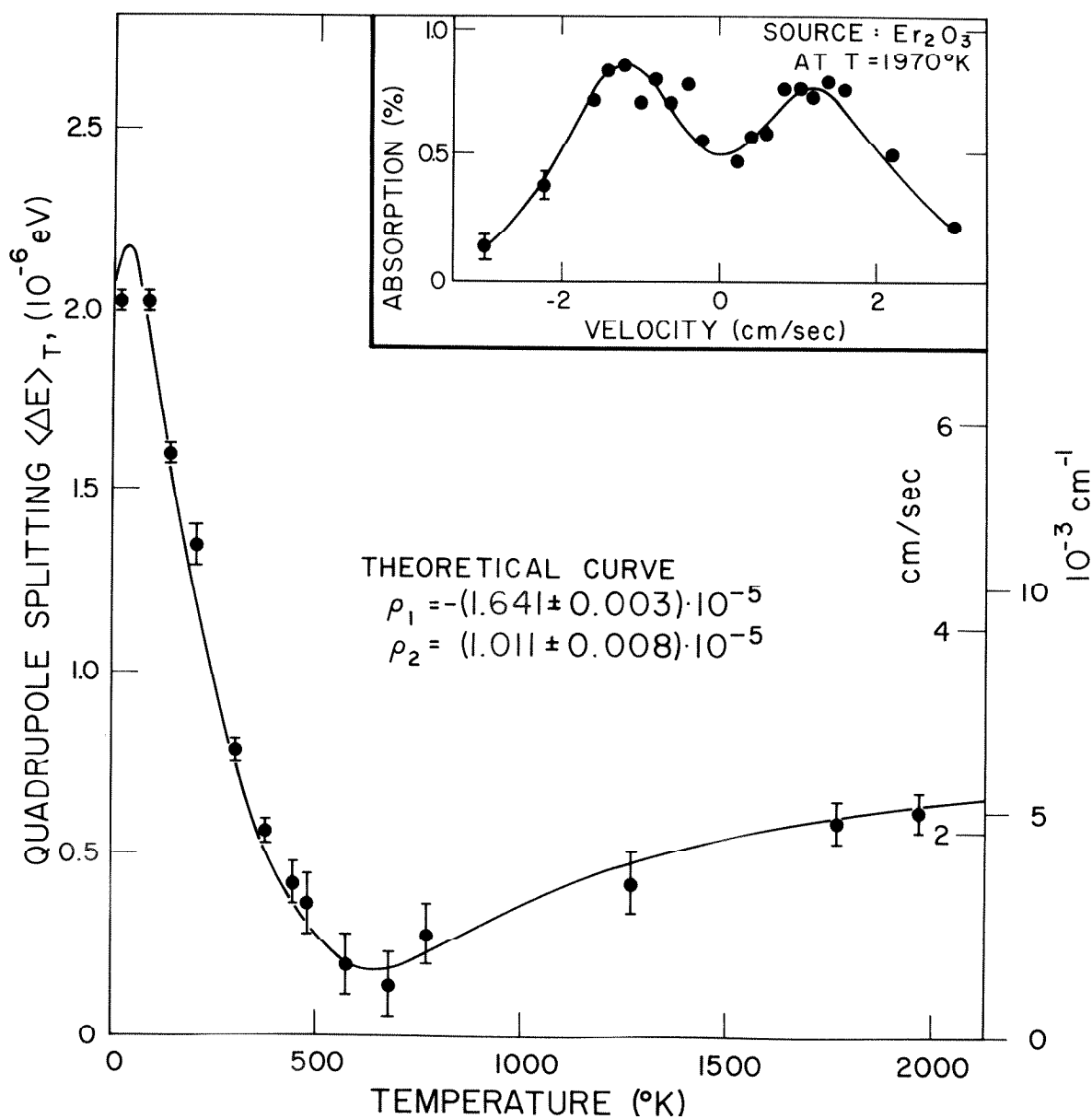


FIG. 11.

axially symmetric electric field gradient at the nucleus, i. e.

$\langle \underline{q}_{xx} - \underline{q}_{yy} \rangle_T = 0$. In this case the quadrupole splitting $\langle \Delta E \rangle_T$ of the gamma lines, Eq.(23), reduces to

$$\langle \Delta E \rangle_T = \frac{1}{2} C_2^0 [\rho_1 \langle 3 \underline{J}_z^2 - \underline{J}^2 \rangle_T + 4 \rho_2] \quad (24)$$

Method 1: In order to obtain the quantities C_2^0 and $\langle 3 \underline{J}_z^2 - \underline{J}^2 \rangle_T$ entering in Eq.(24) we use different sets of optically determined CEF parameters given in Table II. Set 1 was obtained for Tm^{3+} in LaES by Wong and Richman (14), who employed observed optical levels from a series of different optical multiplets. Set 2 was obtained for Tm^{3+} in TmES by Gruber and Krupke (15), who again used observed optical levels from a series of different optical multiplets. In contrast, set 3 was obtained by a least-squares method using only levels observed by Gruber and Krupke (15) in the $^3\text{H}_6$ term of Tm^{3+} in TmES. The evaluation of the C_n^m given in set 3 thus does not employ optical terms other than $^3\text{H}_6$ and therefore should be the set most appropriate for our reduction of the nuclear quadrupole measurements. To permit a check on the intrinsic consistency obtainable by using one set of CEF parameters for the whole series of optical levels we confront in Table III observed and calculated CEF levels. The overall agreement is rather encouraging, the average deviations between calculated and observed values being only of the order of experimental uncertainties. Table IV gives for set 3 the wave functions and field gradients for the CEF levels which are necessary for the evaluation of the temperature average

TABLE II

CEF parameters C_n^m for thulium ethyl sulfate (units cm^{-1})

Set number	C_2^0	C_4^0	C_6^0	C_6^6	References
1	129.8	-71.0	-28.6	432.8	Wong and Richman (14)
2	135.2	-71.3	-28.8	428.1	Gruber and Krupke (15)
3	130.5	-65.9	-28.6	427.3	See text

TABLE III

Observed and calculated CEF levels for thulium ethyl sulfate in the 3H_6 term of the ground multiplet (units cm^{-1}). The calculated levels of set 1 were taken from Wong and Richman (14). For sets 2 and 3 the following reduced matrix elements were used (15):

$$\begin{aligned} \langle J \parallel \alpha \parallel J \rangle &= 1.0197 \cdot 10^{-2}, & \langle J \parallel \beta \parallel J \rangle &= 1.5938 \cdot 10^{-4} \quad \text{and} \\ \langle J \parallel \gamma \parallel J \rangle &= -5.5318 \cdot 10^{-6}. \end{aligned}$$

Observed levels ^a	Calculated levels ^b		
	Set 1	Set 2	Set 3
302.5	306.8	304.7	300.8
274.0	281.1	279.7	274.3
	219.3	221.2	221.7
	212.9	215.1	215.5
198.9	204.3	204.0	198.8
157.3	162.1	161.4	157.8
110.9	113.3	111.5	110.7
32.1	32.1	28.9	32.0
0	-0.5	-4.4	0.7

a Optically determined levels of Gruber and Krupe (15)

b Calculated levels using the CEF parameters given in Table II. The center of gravity of the calculated levels is adjusted to give the best fit.

TABLE IV

Energies, wave functions and electric field gradients of the CEF levels of the 3H_6 term of the ground multiplet of thulium ethyl sulfate (C_{3h} symmetry), using the CEF parameters of set 3 and the reduced matrix elements given in the caption of Table III.

Energy	Degeneracy	Wave Function ^a	$3J_z^2 - J^2$
137.1	1	$-0.707 \mid -3 \rangle + 0.707 \mid + 3 \rangle$	-15.0
110.6	2	$-0.446 \mid -2 \rangle + 0.895 \mid + 4 \rangle$ $0.895 \mid -4 \rangle - 0.446 \mid + 2 \rangle$	- 1.1
58.0	1	$0.697 \mid -6 \rangle - 0.168 \mid 0 \rangle + 0.697 \mid + 6 \rangle$	63.0
51.8	1	$-0.707 \mid -6 \rangle + 0.707 \mid + 6 \rangle$	66.0
35.1	2	$-0.305 \mid -1 \rangle + 0.953 \mid + 5 \rangle$ $-0.953 \mid -5 \rangle + 0.305 \mid + 1 \rangle$	26.3
-5.9	1	$0.707 \mid -3 \rangle + 0.707 \mid + 3 \rangle$	-15.0
-53.0	2	$0.895 \mid -2 \rangle + 0.446 \mid + 4 \rangle$ $0.446 \mid -4 \rangle + 0.895 \mid + 2 \rangle$	-22.9
-131.7	2	$0.305 \mid -5 \rangle + 0.953 \mid + 1 \rangle$ $0.953 \mid -1 \rangle + 0.305 \mid + 5 \rangle$	-32.3
-163.0	1	$0.119 \mid -6 \rangle + 0.986 \mid 0 \rangle + 0.119 \mid + 6 \rangle$	-39.0

a The general form of the wavefunction is given in Eq. (9)

$\langle 3\tilde{J}_Z^2 - \tilde{J}^2 \rangle_T$, Eqs. (16) and (24).

A summary of the reduced data obtained by combining our measurements of the temperature dependence of the nuclear quadrupole interaction for Tm^{3+} in TmES with the results of optical measurements performed on the same compound is presented in Table V. The dimensionless parameters ρ_1 and ρ_2 presented in Table V are experimentally obtained quantities (compare Fig. 10 curve A) which hold within the framework of the CEF model. The advantage of introducing these parameters is that their deduction does not depend on a knowledge of the radial distribution of the 4f-electrons or the value of the nuclear quadrupole moment. Such a knowledge, however, enters into the evaluation of the shielding factors, Eqs. (22), (21) and (5).

Method 2: At elevated temperatures the temperature average $\langle 3\tilde{J}_Z^2 - \tilde{J}^2 \rangle_T$ entering in Eq. (24) may be approximated by Eq. (I-17) of Appendix I, which yields $\langle 3\tilde{J}_Z^2 - \tilde{J}^2 \rangle_T = -14.1 C_2^0/kT$. Expansion (I-17), which applies to the case of an axially symmetric field gradient, was first given by Elliott (39). Details are given in Appendix I, which also includes an extension to the case of non-axially symmetric field gradients. From a plot as a function of $1/T$ of our measurements obtained for TmES at temperatures $T > 200^\circ\text{K}$, Fig. 12, we obtain from Eqs. (24) and (I-17) the values $\rho_1 (C_2^0)^2 = (0.18 \pm 0.05) \text{cm}^{-2}$ and $\rho_2 C_2^0 = (2.8 \pm 1.1) 10^{-3} \text{cm}^{-1}$. These values may be compared

(38) M. C. Olsson and B. Elbek, Nuclear Phys. 15, 134 (1960)

(39) R. J. Elliott, Rev. Mod. Phys. 36, 385 (1964) and private communication

TABLE V

Reduced data for Tm^{3+} in TmES and in Tm_2O_3 . The dimensionless parameters ρ_1 and ρ_2 were obtained in the case of method 1 by a least-squares fit of $\langle \Delta E \rangle_T$, Eq.(23), to the experimental data points given in Figs. 10 and 11. Similarly, in the case of method 2 the parameters ρ_1 and ρ_2 were obtained by fitting Eq.(23) to the experimental data points, using the approximations of Appendix I in the range of their validity, compare Fig. 12. Atomic units are used throughout the table. The errors stated in columns 4 and 5 are only errors arising from our measurements of the nuclear quadrupole interaction and do not include uncertainties in the optical measurements.

Compound	Method	Set	ρ_1	ρ_2	$\langle r^{-3} \rangle_Q^a$	$(1-\gamma_{\infty})/\langle r^2 \rangle_E^a$
TmES	1	1	$(9.34 \pm 0.05) \cdot 10^{-6}$	$(2.08 \pm 0.05) \cdot 10^{-5}$	10.1	388
TmES	1	2	$(9.07 \pm 0.05) \cdot 10^{-6}$	$(2.17 \pm 0.05) \cdot 10^{-5}$	10.2	405
TmES	1	3	$(9.22 \pm 0.05) \cdot 10^{-6}$	$(1.97 \pm 0.05) \cdot 10^{-5}$	10.0	368
TmES	2	3	$(10 \pm 3) \cdot 10^{-6}$	$(2.1 \pm 0.8) \cdot 10^{-5}$	11	390
Tm_2O_3	1	-	$-(1.641 \pm 0.003) \cdot 10^{-5}$	$(1.011 \pm 0.008) \cdot 10^{-5}$	11.3	187
Tm_2O_3	2	-	$-(1.7 \pm 0.9) \cdot 10^{-5}$	$(1.0 \pm 0.2) \cdot 10^{-5}$	11.6	190

^a Using the theoretical value $Q = 1.5$ barn for the nuclear quadrupole moment of the 8.4 keV state of Tm-169 from Oleson and Elbek (38)

Fig. 12: Nuclear quadrupole interaction of Tm^{169} in absorbers of thulium ethyl sulfate and thulium oxide plotted as a function of $1/T$ in the high temperature ranges where method 2 is applicable (see text). The straight lines are the best fit to the experimental data points.

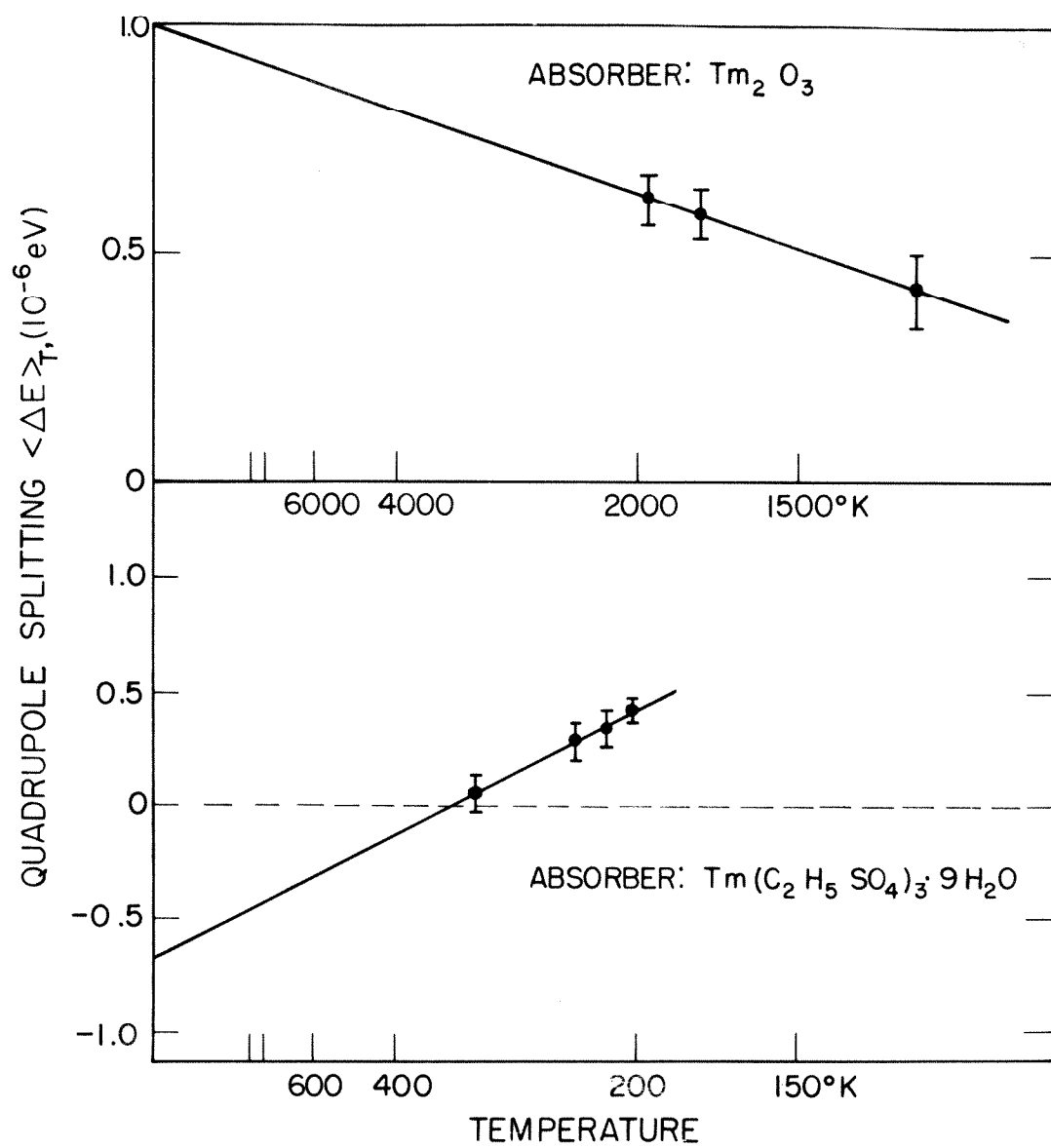


FIG. 12.

with the values obtained by method 1: $\rho_1(C_2^0)^2 = (0.157 \pm 0.001) \text{ cm}^{-2}$ and $\rho_2 C_2^0 = (2.57 \pm 0.07) 10^{-3} \text{ cm}^{-1}$. The agreement between these two values obtained by two different methods gives confidence in the consistency of our analysis. In particular we conclude on this basis, that our results are not seriously influenced by any temperature dependence of the CEF parameters C_n^m , within the temperature range studied ($9.6^\circ \text{K} - 300^\circ \text{K}$). The agreement obtained for the results of methods 1 and 2 indicates that the CEF parameter C_2^0 is reasonably independent of temperature. The higher order parameters C_4^0 , C_6^0 and C_6^6 should be even less dependent on temperature, because of the faster convergence of the associated lattice sums. The justification of the neglect of any temperature dependence of the CEF parameters C_n^m in our analysis is supported by measurements of Gruber and Conway (40), who determined by optical methods the energies of CEF levels of Tm^{3+} ions in TmES at $T = 77^\circ \text{K}$, 194°K and 273°K . The changes with temperature in the position of the levels typically are less than 10 cm^{-1} . We therefore feel justified in using in our analysis one set of CEF parameters, C_n^m , determined optically at a single temperature.

2. Thulium Oxide (Tm_2O_3)

The Tm^{3+} ions in the Tm_2O_3 (space group T_h^7) occupy two non-equivalent lattice sites; sites with symmetry C_2 and C_{3i} occur in

(40) J. B. Gruber and J. G. Conway, J. Chem. Phys. 32, 1178 (1960)

the ratio 3:1. Experimentally, only the higher populated ionic sites associated with point group symmetry C_2 are observed. By choosing a proper coordinate system the relevant crystal field parameters for C_2 symmetry are limited to $C_2^0, C_2^2, C_4^0, C_4^2, C_4^{-2}, C_4^4, C_4^{-4}, C_6^0, C_6^2, C_6^{-2}, C_6^4, C_6^{-4}, C_6^6, C_6^{-6}$. The parameter C_2^{-2} has been eliminated by the proper choice of the coordinate system. One may always eliminate one C_n^{-m} by such a choice (22) when C_n^m also exists. Assume that in a given coordinate system both C_n^m and C_n^{-m} exist. Then by rotating the coordinate systems about the Z-axis by an angle δ defined by

$$\tan \delta = -C_n^{-m}/C_n^m$$

one may reduce the problem to one parameter in the new coordinate system, $C_n'^m$, which is related to the old parameters by

$$C_n'^m = \sqrt{(C_n^m)^2 + (C_n^{-m})^2}$$

The quadrupole splitting of the gamma lines produced by the non-axially symmetric field gradient is given by Eq.(23).

Method 1: Gruber et al. (16) have studied the optical absorption and emission spectra of Tm^{3+} ions in Y_2O_3 at the C_2 symmetry sites; the same CEF levels were obtained in preliminary studies of Tm^{3+} in Tm_2O_3 , within the limits of the experimental accuracy. Using the energy levels obtained for diluted Tm^{3+} by Gruber et al. (16) we have calculated the crystal field parameters C_n^{II} which are included in Table VI. This calculation was performed by minimizing χ^2 ,

TABLE VI

Observed and calculated crystal field levels for Tm^{3+} in thulium oxide at sites with C_2 symmetry, in the 3H_6 term of the ground multiplet (units cm^{-1}). The following set of CEF parameters was used^a: $C_2^0 = -82$, $C_2^2 = -636$, $C_4^0 = -100$, $C_4^2 = -1070$, $C_4^{-2} = 118$, $C_4^4 = 837$, $C_4^{-4} = -68$, $C_6^0 = 3$, $C_6^2 = 83$, $C_6^{-2} = 2$, $C_6^4 = 227$, $C_6^{-4} = -316$, $C_6^6 = 1$, $C_6^{-6} = 154$

Calculated levels	Observed levels ^b	Degeneracy	Calculated Field Gradients	
			$\langle 3J_z^2 - J^2 \rangle$	$\langle J_+^2 + J_-^2 \rangle$
770	796.9	1	- 1.1	-74.2
768	788.5	1	- 4.1	-69.9
680		1	16.8	-43.0
674		1	7.5	-37.9
497	494.0	1	- 8.7	42.0
429	435.7	1	-21.3	17.5
344		1	-22.2	- 2.3
336	340.0	1	-17.1	25.0
258	230.3	1	- 8.3	11.8
200	219.0	1	3.0	22.7
95	89.3	1	- 9.9	42.7
44	30.7	1	40.3	28.2
- 1	0	1	25.2	37.5

a A preliminary set from Gruber et al. (16)

b From Gruber et al. (16)

using the technique described by Davidon (41). A summary of the reduced data obtained by combining our gamma resonance measurements for Tm^{3+} in Tm_2O_3 (compare Fig. 11) with the results of the optical measurements is included in Table V.

Method 2: At elevated temperatures the temperature averages

$\langle 3J_z^2 - J^2 \rangle_T$ and $\langle J_+^2 + J_-^2 \rangle_T$ entering in Eq.(23) may in first order be approximated by the expressions given in Eq.(I-17) and (I-18) of Appendix I, which yield $\langle 3J_z^2 - J^2 \rangle_T = -14.1 C_2^0/kT$ and $\langle J_+^2 + J_-^2 \rangle_T = -9.4 C_2^2/kT$. From a plot as a function of $1/T$ of our measurements

obtained from Tm_2O_3 at temperatures $T \geq 1270^\circ\text{K}$, Fig. 12, we obtain by using Eqs.(23), (I-17), (I-18) the following values:

$$\rho_1 C_2^0 [(C_2^0)^2 + \frac{1}{3}(C_2^2)^2]^{\frac{1}{2}} = (0.5 \pm 0.3) \text{ cm}^{-2} \quad \text{and} \quad \rho_2 [(C_2^0)^2 + \frac{1}{3}(C_2^2)^2] = (4.0 \pm 0.9) 10^{-3} \text{ cm}^{-1}$$

These two values again may be compared with the corresponding values obtained by method 1, namely $(0.508 \pm 0.001) \text{ cm}^{-2}$ and $(3.80 \pm 0.03) 10^{-3} \text{ cm}^{-1}$, respectively. The rather good agreement between the values obtained by methods 1 and 2 suggests, as in the case of TmES , that the neglect in our analysis of any temperature dependence of the CEF parameters C_n^m is a justifiable approximation. Furthermore, the agreement suggests the absence of crystallographic phase transitions in the whole temperature range studied. X-ray diffraction studies of Stecura and Campbell (42) do not reveal any phase transitions within the temperature range $300^\circ\text{K} < T < 1568^\circ\text{K}$.

(41) W.C. Davidon, ANL-Report 5990 rev., (Nov. 1959)

(42) S. Stecura and W.J. Campbell, U.S. Bur. Mines, Rept. on Investigation No. 5847 (1961)

VI. ELECTRONIC SHIELDING FACTORS

Our experiments reveal the presence of strong charge polarizations of closed electron shells. The shielding (or antishielding) factors R_Q , γ_∞ and σ_2 , which were introduced in Sections II and III, are a measure of these charge polarizations.

The antishielding factor γ_∞ ("lattice" Sternheimer factor) may be calculated by several techniques when the free ion wavefunctions are known. Wikner and Burns (25), Ray (26), Sternheimer (27), and Freeman and Watson (28) have made calculations of this quantity for certain rare earth ions, and their results are summarized in Table VII. Wikner and Burns used the (restricted) Hartree-Fock wavefunctions calculated by Ridley (43) for Pr^{3+} and Tm^{3+} and calculated γ_∞ by means of a perturbation-variation method. Sternheimer used the same wavefunctions, but calculated γ_∞ by direct solution of the inhomogeneous Schrödinger equation for the perturbed wavefunctions. Freeman and Watson used the unrestricted Hartree-Fock formalism to calculate γ_∞ for Ce^{3+} . The value of Freeman and Watson for Ce^{3+} is not very different from that obtained by Sternheimer for the neighboring ion Pr^{3+} , but differs appreciably from the value which Wikner and Burns obtained for Pr^{3+} .

Theoretical evaluations of the shielding factor R_Q are more involved. This results because of the proximity of the closed electron shells to the distorting source, the 4f-electrons. For this reason, one may even expect that the distorted shells may produce

(43) E. C. Ridley, Proc. Cambridge Phil. Soc. 56, 41 (1960)

repercussions upon the 4f-electron shell, as was pointed out by Freeman and Watson (12), (44). Table VII includes the few available theoretical values of $R_Q = R_{\text{rad}} + R_{\text{ang}}$ for rare earth ions.

Theoretical evaluations of the shielding factor σ_2 are physically similar to those for γ_∞ . The additional complication arises from the fact, that γ_∞ is a measure of the closed shell distortions experienced at the origin, while σ_2 is a measure of the closed shell distortions experienced at the position of the 4f-electrons, thus requiring in addition a rather precise knowledge of the 4f-electron density. Theoretical predictions for σ_2 are still rather qualitative. Lenander and Wong (10) came to the conclusion that the shielding factor σ_2 was of the order of 0.5 to 0.75 in the case of PrCl_3 while Watson and Freeman (12) in the case of cerium ions likewise concluded that shielding via the σ_2 factor is large. Ray (26) arrives at the theoretical value of $\sigma_2 = 0.52$ for the case of PrCl_3 . Burns (9), on the other hand, using analytic perturbation calculations, concludes that the shielding factor σ_2 should be at most of the order of 0.1 for rare earth ions.

The analysis of our experimental results yields the parameters ρ_1 and ρ_2 given in Table V. Using the value of the nuclear quadrupole moment Q we can evaluate the parameters $\langle r^{-3} \rangle_Q$ and $(1-\gamma_\infty)/\langle r^2 \rangle_E$. Values of these parameters are included in Table V. It appeared reasonable to use a theoretical value for γ_∞ to obtain the radial integral $\langle r^2 \rangle_E$, since theoretical evaluations of this quantity

(44) A. J. Freeman and R. E. Watson, Phys. Rev. 131, 2566 (1963)

TABLE VII

Theoretical values of Sternheimer shielding factors for rare earth ions

Ion	γ_{∞}	R_{rad}	R_{ang}	Reference
Ce ³⁺	- 73.5	-0.43 ^a		(28)
Pr ³⁺	- 16.4			(26)
Pr ³⁺	-105			(25)
Pr ³⁺	- 78.5			(27)
Tm ³⁺	- 61.5			(25)
Tm ³⁺	- 74			(27)
Eu ³⁺			0.29	(5)

a Using the value (28) $\langle r^{-3} \rangle_{4f} = 4.71 \text{ a.u.}$

appear to be relatively reliable.

Besides the values of the "electric" radial integrals $\langle r^{-3} \rangle_Q$ and $\langle r^2 \rangle_E$, which enter in the analysis of our measurements of the nuclear quadrupole interaction, there exists a "magnetic" radial integral $\langle r^{-3} \rangle_M$, which enters in the analysis of nuclear magnetic interactions. The effective integral $\langle r^{-3} \rangle_M$ likewise may be associated with a shielding factor (5), (45), which in analogy with the electric case is defined through the relation $\langle r^{-3} \rangle_M = \langle r^{-3} \rangle_{4f} (1 - R_M)$ (compare Eq.(21)). The difference between the values of $\langle r^{-3} \rangle_Q$ and $\langle r^{-3} \rangle_M$ arises because the contributions from the closed shells differ for the quadrupole and the magnetic interactions. This difference is due to the different forms of the interaction operators for the nuclear quadrupole, magnetic orbital and magnetic spin interactions, as was emphasized by Sternheimer (5), (45) and Freeman and Watson (44).

The radial integrals $\langle r^{-3} \rangle_Q$, $\langle r^{-3} \rangle_M$ and $\langle r^2 \rangle_E$, which enter the nuclear quadrupole, nuclear magnetic and CEF interactions, incorporate the contributions to these interactions from both the partially filled (4f) and the closed electron shells. These radial integrals in principle may be taken from experimental observations, a procedure adopted in this paper. Table VIII includes a compilation of relevant

-
- (45) R. Sternheimer, Phys. Rev. 86, 316 (1952)
 - (46) I. Lindgren, Nuclear Phys. 32, 151 (1962)
 - (47) B. R. Judd and I. Lindgren, Phys. Rev. 122, 1802 (1961)
 - (48) R. L. Cohen, Phys. Rev. 134, A94 (1964)
 - (49) E. Gerdau, W. Krull, L. Mayer, J. Braunsfurth, J. Heisenberg, P. Steiner, E. Bodenstedt, Z. Physik 174, 389 (1963)

radial integrals for Tm^{3+} ions in different chemical surroundings, obtained from experimental data by using the theoretical values for Q and γ_{∞} given in the caption. The table includes radial integrals evaluated from our gamma resonance studies as well as from other pertinent experiments.

The interpretation of the radial integrals in terms of electronic shielding factors requires a knowledge of the quantities $\langle r^{-3} \rangle_{4f}$ and $\langle r^2 \rangle_{4f}$, as discussed above. These radial integrals are not accessible to direct experimental observation and one is forced to use theoretical values, the evaluation of which is presently somewhat uncertain because of the lack of sufficiently accurate atomic wave functions for rare earth ions. Any evaluation of electronic shielding factors is therefore limited by the uncertainties in these theoretical values. Nevertheless, by using a specific set of theoretical values throughout the whole analysis, one still can observe the general trend in electronic shielding.

Freeman and Watson (50) discuss the theoretical situation in the evaluation of $\langle r^{-3} \rangle_{4f}$ and $\langle r^2 \rangle_{4f}$ for most rare earth ions. These authors, in particular, have shown that the values of $\langle r^{-3} \rangle_{4f}$ for rare earth ions incorporated in a solid do not differ very much from the free ion values (28). Table VIII includes a compilation of electronic shielding factors for Tm^{3+} ions obtained by using the theoretical quantities given in the caption. The uncertainties of the theoretical values of Q , $\langle r^2 \rangle_{4f}$ and $\langle r^{-3} \rangle_{4f}$ are presumably less than 30%.

(50) A. J. Freeman and R. E. Watson, Phys. Rev. 127, 2058 (1962)

TABLE VIII

Semi-experimental electronic shielding factors for Tm^{3+} . The values of columns 2 and 6 are taken from Table V. The following theoretical values were used in the table: $\langle r^{-3} \rangle_{4f} = 11.20$ from Lindgren (46) (columns 3, 5); $\langle r^2 \rangle_{4f} = 0.68$ from Judd and Lindgren (47) (column 7); $\langle J \| \alpha \| J \rangle = 0.0102$ from several authors (14)-(16), (20) (columns 2, 3); $Q = 1.5$ barn from Oleson and Elbek (38) (columns 2, 3, 6, 7); $\gamma_{\infty} = -74$ from Sternheimer (27) (columns 6, 7). Atomic units are used throughout the table.

Compound	$\langle r^{-3} \rangle_Q$	R_Q	$\langle r^{-3} \rangle_M$	R_M	$\langle r^2 \rangle_E$	σ_2	Reference
TmES^a	10.0	0.107			0.20	0.71	this paper
Tm_2O_3^b	11.3	-0.005			0.40	0.41	this paper
TmFe_2	9.0 ^c	0.196	12.5	-0.116			Cohen (48)
free Tm^{3+} ion			11.73	-0.047			Gerdau et al.(49)

a Using the data obtained by method 1, set 3

b Using the data obtained by method 1

c Evaluated from Cohen's experimental data, using $Q = 1.5$ barn

It appears from Table VIII that the shielding of the nuclear quadrupole interaction and the nuclear magnetic interaction, expressed through the shielding factors R_Q and R_M , is always small in the case of Tm^{3+} ions.

As concerns shielding factors other than R , we note again that our experiments provide only the ratio $(1-\gamma_\infty)/\langle r^2 \rangle_E = (1-\gamma_\infty)/[(1-\sigma_2)\langle r^2 \rangle_{4f}]$, compare Eqs. (22), (23). It appears from column 7 of Table VIII that there is a substantial electronic shielding associated with the shielding factor σ_2 , which describes the fact that the 4f electrons do not interact with the direct CEF, but with a CEF shielded by core electrons (primarily $5s^2 5p^6$ electrons). This experimental observation is in qualitative agreement with conclusions we draw for praseodymium salts from NMR measurements on lanthanum salts performed by Edmonds (6). CEF shielding effects of comparable magnitude were also obtained by Blok and Shirley (8), in the case of several rare earth ethyl sulfates and rare earth double nitrates, using nuclear alignment techniques. We note that our conclusions concerning σ_2 are in agreement with the theoretical estimates of Lenander and Wong (10), Ray (11) and Watson and Freeman (12), but are in serious disagreement with theoretical conclusions of Burns (9).

It is interesting to note the difference in the σ_2 values presented in Table VIII for $TmES$ and Tm_2O_3 . This seems to indicate that σ_2 depends on the chemical environment, which might result from different amounts of overlap of ligand wavefunctions with the central rare earth ion. This seems to conform with similar conclusions by

Hutchings and Ray (21) for the case of PrCl_3 and PrBr_3 . It should be observed that our conclusions concerning σ_2 are based on the plausible assumption that γ_∞ is much less dependent on the chemical bond than σ_2 .

Furthermore, we emphasize that we have neglected the non-linear shielding effects (12) in our analysis. Appreciable non-linear shielding would invalidate the CEF parameterization scheme. However, due to the overall agreement reached in our analysis -- in terms of linear shielding -- of the optical data and our quadrupole data we conclude that non-linear shielding effects play only a minor role.

Similar measurements of the nuclear quadrupole interaction in TmES as those reported in this paper were performed by Hühner et al. (51). Hühner et al. in the analysis of their data did not take into account, that the optically determined CEF parameter C_2^0 does not represent an unshielded CEF parameter but rather represents a potential at the 4f-electron sites which undergoes shielding by closed electron shells of the order of 70%, as shown in this paper. We would like to emphasize, in this context, that the lattice contribution to the total electric field gradient at the nuclear sites is most easily observed in the measurements performed at higher temperatures.

The nuclear quadrupole interaction in Tm_2O_3 has been investigated previously in a limited temperature range by Cohen et al. (23)

(51) S. Hühner, M. Kalvius, P. Kienle, W. Wiedemann, H. Eicher, Z. Physik 175, 416 (1963)

and Kalvius et al. (52) using recoilless resonance absorption of gamma rays. In the analyses of these papers the direct contribution from the lattice to the electric field gradient, enhanced by electronic shielding, was not considered. Preliminary results for Tm_2O_3 in a limited temperature range were reported by Cohen (53).

Although the importance of shielding effects expressed by the factor σ_2 is well established, the absolute values of the shielding factor σ_2 may be in error by up to 30%. On these grounds we do not feel that there exists any of the serious discrepancies reported by Hufner et al. (51) between the value of the nuclear quadrupole moments obtained by gamma resonance measurements and those derived from Coulomb excitation measurements.

-
- (52) M. Kalvius, W. Wiedemann, R. Koch, P. Kienle and H. Eicher, Z. Physik 170, 267 (1962)
- (53) R. L. Cohen, Ph.D. thesis, Department of Physics, California Institute of Technology, Pasadena, 1962, unpublished

VII. SUMMARY

This work has demonstrated that the technique of gamma resonance absorption provides a sensitive method for investigating electronic shielding by closed electron shells in rare earths, via measurements of the temperature dependence of the nuclear hyperfine interactions. It was shown, in particular, that in those cases where measurements can be performed at elevated temperatures one can obtain information on electronic shielding factors without the necessity of relying on CEF parameters determined by other methods, such as optical spectroscopy. Our results lead to the conclusion that the distortions induced in the closed electron shells by the 4f shell only produce a small shielding of the 4f electron contribution to the total field gradient at the nuclear site ("atomic" Sternheimer shielding factor $|R_Q| \lesssim 0.1$). On the other hand the distortions induced in the closed electron shells by the CEF lead to substantial enhancement of the direct electric field gradient produced by the surrounding ions at the nuclear site ("lattice" Sternheimer antishielding factor γ_∞) as well as to a substantial reduction of the CEF as seen by the 4f-electrons (shielding factor σ_2). We obtain values for $(1-\gamma_\infty)/(1-\sigma_2)$ of 250 for Tm^{3+} ions in thulium ethyl sulfate and of 128 for Tm^{3+} in thulium oxide. The difference in these two values seems to demonstrate a dependence on the chemical bond.

It is interesting to note that the ratio of $1-\sigma_2$ for TmES to $1-\sigma_2$ for Tm_2O_3 agrees approximately with the ratio of the overall CEF splittings in these two compounds.

It appears that measurements of the nuclear quadrupole inter-

action are presently much better suited to determine electronic shielding factors than to determine nuclear quadrupole moments, due to the existing uncertainties in the different electronic shielding phenomena.

APPENDIX I

In what follows we derive an approximation for the electric field gradient which holds at elevated temperatures.

The relevant matrix elements entering the expression for the electric field gradient introduced in the text, Eq.(15) can be expressed in terms of spherical harmonics by

$$\langle J || \alpha || J \rangle \langle 3 J_z^2 - J^2 \rangle_T = 4\sqrt{\pi/5} \langle \sum_i Y_2^0(\vartheta_i, \varphi_i) \rangle_T \quad (\text{I-1a})$$

$$(\text{I-1b})$$

$$\langle J || \alpha || J \rangle \langle J_+^2 + J_-^2 \rangle_T = 4\sqrt{2\pi/15} \langle \sum_i [Y_2^2(\vartheta_i, \varphi_i) + Y_2^{-2}(\vartheta_i, \varphi_i)] \rangle_T$$

where the \sum_i extends over all 4f electrons.

Using the density matrix formalism the thermal average of the spherical harmonics in Eq.(I-1) may be written as

$$\langle Y_n^m \rangle_T = Z^{-1} \sum_{\lambda M} \langle \lambda M | Y_n^m \exp [-\beta (H_0 + V)] | \lambda M \rangle \quad (\text{I-2})$$

where

$$Z = \sum_{\lambda M} \langle \lambda M | \exp [-\beta (H_0 + V)] | \lambda M \rangle \quad (\text{I-3})$$

and $\beta = 1/kT$. The Coulomb and spin-orbit interactions are represented by H_0 and V is the CEF potential defined by

$$V = \sum_{i n m} a_n^m r_i^n Y_n^m(\vartheta_i, \varphi_i) \quad (I-4)$$

and the electronic wave functions $|\lambda \nu\rangle$ for pure Russell-Saunders coupling are defined by

$$(H_0 + V) |\lambda \nu\rangle = (E_\lambda + E_\nu) |\lambda \nu\rangle \quad (I-5)$$

The quantum numbers α LSJ are represented by λ and ν is a quantum number characterizing the CEF levels. Since the trace of a matrix is invariant to the choice of basis functions, we choose eigenfunctions of \tilde{J}_Z in Eqs.(I-2) and (I-3) rather than using the eigenfunctions in Eq.(I-5) which are mixed in M. The "lattice sums" a_n^m introduced in Eq.(I-4) are linear functions of those used in the text (compare Eq.(1)). We have for instance

$$a_2^0 = 4\sqrt{\pi/5} A_2^0 \quad (I-6a)$$

$$a_2^2 + a_2^{-2} = 4\sqrt{2\pi/15} A_2^2 \quad (I-6b)$$

and we choose $a_0^0 = 0$.

According to Van Hove et al. (54) the exponential factor in Eqs.(I-2) and (I-3) may be expanded as follows

(54) L. Van Hove, N.M. Hugenholtz, L.P. Howland, Quantum Theory of Many Particle Systems (W.A. Benjamin, Inc., New York 1961) p. 82

$$\exp [-\beta (H_0 + V)] = \sum_{n=0}^{\infty} \rho_n \quad (I-7)$$

where $\rho_0 = \exp(-\beta H_0)$ and for $n > 0$ we have

$$\rho_n = (-1)^n \int_0^\beta d\beta_1 \int_0^{\beta_1} d\beta_2 \dots \int_0^{\beta_{n-1}} d\beta_n \exp [-(\beta - \beta_1) H_0] V \cdot$$

$$\cdot \exp [-(\beta_1 - \beta_2) H_0] V \dots V \exp [-(\beta_{n-1} - \beta_{n-2}) H_0] V \exp (-\beta_n H_0)$$

For a temperature large compared with the CEF interaction energy (i. e. $\beta E_V < 1$) only the first few terms of Eq. (I-7) need be considered.

Hence Eq. (I-2) reduces to

$$(I-8)$$

$$\langle Y_n^m \rangle_T = Z^{-1} \sum_{\substack{\lambda\lambda' \\ MM'}} \langle \lambda M | Y_n^m | \lambda' M' \rangle \langle \lambda' M' | \rho_0 + \rho_1 + O(\beta^2) | \lambda M \rangle$$

where

$$Z = \sum_{\lambda M} \langle \lambda M | \rho_0 + \rho_1 + O(\beta^2) | \lambda M \rangle$$

and

$$\langle \lambda' M' | \rho_0 | \lambda M \rangle = \exp(-\beta E_\lambda) \delta_{\lambda\lambda'} \delta_{MM'} ,$$

$$\langle \lambda' M' | \rho_1 | \lambda M \rangle = \begin{cases} -\beta \exp(-\beta E_\lambda) \langle \lambda M' | V | \lambda M \rangle & \text{for } \lambda = \lambda' \\ -\exp(-\beta E_{\lambda'}) \frac{\exp[\beta(E_{\lambda'} - E_\lambda)] - 1}{E_{\lambda'} - E_\lambda} \cdot \langle \lambda' M' | V | \lambda M \rangle & \text{for } \lambda \neq \lambda' \end{cases}$$

Furthermore, if the temperature is also small compared with the spin-orbit splitting (i.e. $\beta(E_{\lambda_1} - E_{\lambda_0}) \gg 1$, where λ_1 represents the first excited term of the ground multiplet and λ_0 represents the ground term) only the ground term is appreciably populated. Thus Eq.(I-8) reduces to

$$\begin{aligned} \langle Y_n^m \rangle_T = -Z^{-1} \sum_{MM'} & \left[\beta \langle \lambda_0 M | Y_n^m | \lambda_0 M' \rangle \langle \lambda_0 M' | V | \lambda_0 M \rangle + \right. \\ & \left. + 2 \sum_{\lambda' \neq \lambda_0} \langle \lambda_0 M | Y_n^m | \lambda' M' \rangle \langle \lambda' M' | V | \lambda_0 M \rangle / E_{\lambda'} \right] \end{aligned} \quad (\text{I-9})$$

for $n > 0$. Here $Z = 2J_0 + 1$ and we have chosen $E_{\lambda_0} = 0$. Furthermore because of the Wigner-Eckart theorem and the properties of the vector coupling coefficients (the notation of Edmonds' (55) is used) we have used the following relations

(55) A. R. Edmonds, Angular Momentum in Quantum Mechanics (Princeton University Press, Princeton, 1957)

$$\sum_M \langle \lambda M | Y_n^m | \lambda M \rangle = (2n+1)^{-\frac{1}{2}} \langle \lambda || Y_n || \lambda \rangle \cdot \sum_M (-1)^{J-M} \langle J M J - M | J J n m \rangle$$

$$(-1)^{J-M} = (2J+1)^{\frac{1}{2}} \langle J M J - M | J J 0 0 \rangle$$

$$\sum_M \langle J J 0 0 | J M J - M \rangle \langle J M J - M | J J n m \rangle = \delta_{n 0} \delta_{m 0}$$

and therefore

$$\sum_M \langle \lambda M | Y_n^m | \lambda M \rangle = 0 \quad \text{for } n > 0 \quad (\text{I-10})$$

According to Eq.(I-1) we are only interested in the cases of even n and m , for which we obtain from Eq.(I-9)

$$\langle Y_n^m(\vartheta, \varphi) \rangle_T = -(2J_0 + 1)^{-1} a_n^{-m} \left\{ \langle \lambda_0 || Y_n(\vartheta) || \lambda_0 \rangle \cdot \right.$$

$$\cdot \sum_i \{ \langle r_i^n \rangle \langle \lambda_0 || Y_n^\dagger(\vartheta_i) || \lambda_0 \rangle \}^{\beta+2} \sum_{\lambda' \neq \lambda_0} \left[\langle \lambda_0 || Y_n(\vartheta) || \lambda' \rangle \cdot \right.$$

$$\cdot \sum_i \{ \langle r_i^n \rangle \langle \lambda' || Y_n^\dagger(\vartheta_i) || \lambda_0 \rangle \} (E_{\lambda'})^{-1} \left. \right\} \cdot (2n+1)^{-1} \quad (\text{I-11})$$

In arriving at Eq.(I-11) we used Eq.(I-4) and the following relations:

$$\begin{aligned}
& \sum_{MM'} \langle \lambda_0 M | Y_n^m | \lambda' M' \rangle \langle \lambda' M' | Y_p^q | \lambda_0 M \rangle = \\
& = [(2n+1) (2p+1)]^{\frac{1}{2}} \langle \lambda_0 \| Y_n \| \lambda' \rangle \langle \lambda' \| Y_p \| \lambda_0 \rangle \cdot \\
& \cdot \sum_{MM'} (-1)^{M+M'} \langle J_0 J' n m | J_0 M J' - M' \rangle \langle J' M' J_0 - M | J' J_0 p q \rangle = \\
& = [(2n+1) (2p+1)]^{-\frac{1}{2}} \langle \lambda_0 \| Y_n \| \lambda' \rangle \langle \lambda' \| Y_p \| \lambda_0 \rangle (-1)^m \cdot \\
& \cdot \delta_{np} \delta_{m-q} \Delta(J_0 J' n)
\end{aligned}$$

where $\Delta(J_0 J' n) = 1$ if J_0, J' and n satisfy the triangular condition and Δ is zero otherwise.

Following Elliott and Stevens (18) we now make the following correspondence between reduced matrix elements

$$\langle J \| \alpha \| J \rangle = 4\sqrt{\pi/5} \langle \alpha LSJ \| \sum_i Y_2(\vartheta_i) \| \alpha LSJ \rangle / \sqrt{\Omega_{J,J}} \quad (I-12a)$$

$$\langle J \| \alpha \| J+1 \rangle = -4\sqrt{\pi/5} \langle \alpha LSJ \| \sum_i Y_2(\vartheta_i) \| \alpha LSJ+1 \rangle / \sqrt{\Omega_{J,J+1}} \quad (I-12b)$$

$$\langle J \| \alpha \| J+2 \rangle = 4\sqrt{\pi/5} \langle \alpha LSJ \| \sum_i Y_2(\vartheta_i) \| \alpha LSJ+2 \rangle / \sqrt{\Omega_{J,J+2}} \quad (I-12c)$$

where

$$\Omega_{J,J} = J(J+1)(2J+1)(2J-1)(2J+3) \quad (I-13a)$$

$$\Omega_{J, J+1} = \frac{1}{3} J (J+1) (J+2) (2J+1) (2J+3) \quad (\text{I-13b})$$

$$\Omega_{J, J+2} = \frac{2}{3} (J+1) (J+2) (2J+1) (2J+3) (2J+5) \quad (\text{I-13c})$$

Finally, by combining Eqs. (I-1), (I-6), (I-11) and (I-12) we obtain the following expressions:

$$\langle J \| \alpha \| J \rangle \langle \underline{3J^2 - J^2} \rangle_T = A_2^0 \langle r^2 \rangle_E \Phi(T) \quad (\text{I-14})$$

$$\langle J \| \alpha \| J \rangle \langle \underline{J_+^2 + J_-^2} \rangle_T = \frac{2}{3} A_2^2 \langle r^2 \rangle_E \Phi(T) \quad (\text{I-15})$$

where

$$\begin{aligned} \Phi(T) = -\frac{1}{5} (2J+1)^{-1} & \left[\frac{|\langle J \| \alpha \| J \rangle|^2 \Omega_{JJ}}{kT} - \frac{2 |\langle J \| \alpha \| J \pm 1 \rangle|^2 \Omega_{J, J \pm 1}}{E_{J \pm 1}} \right. \\ & \left. + \frac{2 |\langle J \| \alpha \| J \pm 2 \rangle|^2 \Omega_{J, J \pm 2}}{E_{J \pm 2}} \right] \quad (\text{I-16}) \end{aligned}$$

The factors $\Omega_{J, J-1}$ and $\Omega_{J, J-2}$ in Eq. (I-16) are obtained from Eqs. (I-13b) and (I-13c) by changing J to $J-1$ and $J-2$, respectively. The energies $E_{J \pm 1}$ and $E_{J \pm 2}$ are those of the center of gravity of the terms nearest the ground term which have quantum numbers $J \pm 1$ and $J \pm 2$.

Applying these results to the case of Tm^{3+} , the effect of the second and third terms of Eq.(I-16) is negligible ($< 1\%$) at all temperatures used in our experiments. Under these circumstances we arrive at the following high temperature approximations used in method 2 of the text (compare Eqs.(23) and (24))

$$\langle 3\tilde{J}_z^2 - \tilde{J}^2 \rangle_T = -\frac{1}{5} (2J+1)^{-1} C_2^0 \langle J \parallel \alpha \parallel J \rangle \Omega_{J,J} / kT \quad (\text{I-17})$$

$$\langle \tilde{J}_+^2 + \tilde{J}_-^2 \rangle_T = -\frac{2}{15} (2J+1)^{-1} C_2^2 \langle J \parallel \alpha \parallel J \rangle \Omega_{J,J} / kT \quad (\text{I-18})$$

APPENDIX II

Most of the computations involved in the analysis of the experimental data presented in this paper were carried out with the aid of an IBM 7094 computer. This section contains the listings of the Fortran IV computer programs that were used. The analysis involved four major steps.

1) OPTIC ... A least-squares fitting of the calculated CEF levels, using the method of Section II, to the optically observed levels in terms of the CEF parameters.

2) ICARME ... A calculation of the reduced matrix elements (compare Eqs. (4) and (I-12) in the intermediate coupling approximation starting with the relevant Slater integrals and the spin-orbit coupling parameter.

3) QTAVE ... A least-squares fitting of the calculated nuclear quadrupole splitting, using method 1 of Section V, to the observed splitting in terms of the parameters ρ_1 and ρ_2 .

4) HITEMP ... A least-squares fitting of the calculated nuclear quadrupole splitting, using method 2 of Section V, to the observed splitting at high temperatures.

Some of the programs used are available in the SHARE library and are not included here.

OPTIC

The required card decks are:

- | | | |
|-------------|---|--------------------------------|
| 1. MIN | } | |
| 2. READY | | |
| 3. AIM | | see SHARE no. 980 |
| 4. FIRE | | ZO ANFZO13 |
| 5. DRESS | | |
| 6. STUFF | | |
| 7. MATMPY | | |
| 8. FCN | | |
| 9. THEORY 4 | | |
| 10. QSQUAR | | |
| 11. LEIGEN | | |
| 12. HERM | | see SHARE no. 884 PK HMEE |
| 13. RDM | | see SHARE No. 1359 G5 XGC 0008 |

Decks 1-7 were converted from Fortran II to Fortran IV and
deck 12 was modified so that it could be used with a Fortran program.
The listings of decks 8-12 follow.

```

C      F C N ...
C      THIS SUBROUTINE IS THE LINK BETWEEN THEORY4 AND QSQUAR TO MIN,
C      THE VARIABLE METRIC MINIMAZATION ROUTINE, SHARE NO. 980
C      INPUT DATA
C      PAR(1)=CEF PARAMETERS IN THE FOLLOWING ORDER C20,C22,C40,C42,
C      C4-2,C44,C4-4,C60,C62,C6-2,C64,C6-4,C66,C6-6 UR C20,C40,C60,
C      C66
C      NE=NO. OF ENERGY LEVELS MEASURED
C      ITIME= MAX. XEQ TIME ALLOWED
C      ALOWER=LOWER LIMIT OF RELATIVE DIFFERENCE USED IN CALCULATING
C      GRADIENT
C      UPPER=UPPER LIMIT OF RELATIVE DIFFERENCE USED IN CALCULATING
C      GRADIENT
C      E(1)=MEASURED ENERGY LEVELS
C      R(1)=ERROR IN MEASURED ENERGY LEVELS
C      V(1)=LEVEL IDENTIFICATION
C      DP(1)=STEP SIZE USED FOR GRADIENT
C      AB=IDENTIFICATION FOR PARAMETERS
C      SUBROUTINE FCN(NP,G,F,PAR,MFLAG)
C      COMMON/COMTHE/NFORM,P(3,40)
C      COMMON/COMQSQ/NE,E(100),S(120),R(100)
C      COMMON/COMMIN/H
C      DIMENSION H(40,40),G(40),PAR(40),V(100),DP(40),AB(40)
C      DIMENSION AH(50,22),BH(50,1),FP(40),ITER(40),ITERM(40),DEV(100)
C      IF(MFLAG-1)1,1,2
1      READ(5,100) NE,ITIME,ALOWER,UPPER
100     FORMAT(13 /I6/2E12.5)
C      CALL ICLOCK (INTIME)
C      ITIME=ITIME+INTIME
C      READ(5,800)(E(I),R(I),V(I), I=1,NE)
800     FORMAT(2F20.5,A6)
C      READ(5,200)(DP(I), I=1,NP)
200     FORMAT(F20.5)
C      READ(5,500) AB
500     FORMAT(12A6)
C      READ(5,900)
900     FORMAT(80H  HEADING
1
C      WRITE(6,700) (DP(I), I=1,NP)
700     FORMAT(39HSTEP SIZE USED IN CALCULATING GRADIENT/(3H0  8E14.5))
C      WRITE(6,600) AB
600     FORMAT(23HORDER OF PARAMETERS  X/(20A6))
C      NDEG=NE-NP
2      NFORM=0
C      IF(MFLAG.NE.1) NFORM=1
C      DO 3 I=1,NP
3      P(2,I)=PAR(I)
C      F=0.5*QSQUAR(1,2,2)
C      NFORM=1
C      DO 10 I=1,NP
C      ITERM(I)=0

```

```

ITER(I)=0
12 P(3,I)=PAR(I)*(1.0+DP(I))
   FP(I)=0.5*QSQUAR(I,3,2)
   RF=ABS((FP(I)-F)/(FP(I)+F))
   IF(RF.GT. ALOWER) GO TO 11
   DP(I)= 5.0*DP(I)
   ITER(I)=ITER(I)+1
   IF(ITER(I).LT.9) GO TO 12
   FP(I)=F
   WRITE (6,2001) I,DP(I)
2001 FORMAT(35H0GRADIENT FOR PARAMETER SET TO ZERO 16,E20.8)
   GO TO 10
11 IF(RF.LT. UPPER) GO TO 10
   DP(I)=0.40*DP(I)
   ITERM(I)=ITERM(I)+1
   IF(ITERM(I).LT.9) GO TO 12
   WRITE (6,2002) I,DP(I)
2002 FORMAT(35H0GRADIENT FOR PARAMETER SET TO 10. 16, E20.8)
   FP(I)=F+ 10.0*DP(I)*PAR(I)
10 CONTINUE
   WRITE(6,2000)(ITER(I),ITERM(I), I=1,NP)
2000 FORMAT(30H0DERIVATIVE MOVES**PLUS, MINUS/( 10X,8(I1,1H,I1,11X)))
   WRITE(6,700)(DP(I), I=1,NP)
   DO 4 I=1,NP
4 G(I)=(FP(I)-F)/(DP(I)*PAR(I))
   CALL ICLOCK(LPTIME)
   IF(LPTIME.GT.ITIME) GO TO 50
   IF(MFLAG-3) 60,51,60
50 WRITE(6,1000)
1000 FORMAT(28H0***** TIME EXCEEDED $$$$$$ )
   WRITE(6,1001) (P(2,I), I=1,NP)
1001 FORMAT(32H0RESULTS OF FIT UP TO THIS POINT/3H0X=1P8E14.5/
1 (3H0 8E14.5))
   WRITE(6,1003)
1003 FORMAT(13H0ERROR MATRIX)
   DO 6 I=1,NP
6 WRITE(6,1004)(H(I,J), J=1,NP)
1004 FORMAT(1H01P8E14.5/(1H08E14.5))
   PUNCH 1002,(P(2,I), I=1,NP)
1002 FORMAT(6E12.5)
   DO 5 J=1,NP
5 PUNCH 1002, (H(J,I), I=J,NP)
51 PUNCH 200,(DP(I), I=1,NP)
   CALL THEORY(1,2,2,0)
   WRITE(6,900)
   ANE=NE
   DO 30 I=1,NE
30 DEV(I)=S(I)-E(I)
   STAN=0.0
   DO 31 I=1,NE
31 STAN=STAN+(DEV(I))**2

```

```
      STAN=SQRT(STAN/ANE)
      WRITE(6,901)(S(I),E(I),DEV(I),R(I),V(I), I=1,NE)
901  FORMAT(2F20.3,F11.1,F9.1,15XA6)
      WRITE(6,700)(DP(I), I=1,NP)
      ANODEG=NODEG
      CHI2=2.0*F/ANODEG
      WRITE(6,903) NODEG ,CHI2,STAN
903  FORMAT(30HONUMBER OF DEGREES OF FREEDOM= I6/
134HACHI SQUARED / DEGREES OF FREEDOM= 1PE14.7/
235HORMS DEVIATION FOR EACH LEVEL= +OR- 0PF6.2)
      DO 55 I=1,NP
      DO 55 J=1,NP
      AH(I,J)=H(I,J)
55  AH(J,I)=AH(I,J)
      CALL MATINV(AH,NP,BH,0,DELTA)
      WRITE(6,1005) DELTA
1005 FORMAT(7HDELTA= E20.8)
      IF(LPTIME.GT.ITIME) CALL EXIT
60  RETURN
      END
```

```

C      THEORY 4 ...
C      THIS SUBROUTINE CALCULATES THE ELECTRONIC ENERGY LEVELS OF A RARE
C      EARTH ION IN NTERM TERMS OF THE OPTICAL SPECTRA. THE MAX J=15/2.
C      HIGHER J MAY BE HANDLED IF THE APPROPRIATE DIMENSION STATEMENTS
C      ARE CHANGED. THE LEVELS ARE CALCULATED FROM GIVEN CEF PARAMETERS.
C      NTERM MAX = 20, MAX NO. OF LEVELS = 100, ANY POINT SYMMETRY THAT
C      USES ONLY CEF PARAMETERS WITH EVEN N AND M.
C      INPUT DATA
C      NTERM=NO. OF OPTICAL LSJ TERMS
C      NJ=NO. OF DIFFERENT J VALUES IN TERMS
C      XJ=MIN. J VALUE - 1.0
C      IW=DUMMY VARIABLE
C      IDEG=1 FOR INTEGRAL J, 2 FOR HALF INTEGRAL J
C      DELTA=LIMIT FOR OFF-DIAGONAL ELEMENTS IN EIGENVALUE SUB-
C      ROUTINE EIGENH
C      NRDM=STARTING POINT FOR RANDOM NUMBER FUNCTION RDM
C      SYMTRY=C2 OR C3H AS THE CASE MAY BE
C      C3HSYM=C3H IF THIS IS THE CASE
C      THETA(N,M)=REDUCED MATRIX ELEMENTS, N IS ORDER, M IS TERM
C      IDENTIFICATION
C      AJ(I)=J VALUE FOR THE ITH TERM
C      NOBSVR(M,N)=1 IF THE NTH LEVEL IS NOT OBSERVED AND ZERO
C      OTHERWISE
C      NORMAL(M)=NO. OF THE LEVEL IN THE MTH TERM WHICH IS TO BE
C      NORMALIZED TO ZERO
C      NOP=NO. OF CARDS WITH OPERATOR EQUIVALENT MATRIX ELEMENTS FOR
C      EACH J VALUE DIVIDED BY 3
C      HEAD(K,I)=LABELING FOR EIGENFUNCTIONS
C      FMT(K,J)=FORMAT FOR EIGENFUNCTIONS
C      OA, OB, OC(K,I,J)=IJ OPERATOR EQUIVALENT MATRIX ELEMENT FOR
C      KTH J VALUE FOR ALPHA, BETA, GAMMA RESPECTIVELY, I AND J
C      GO FROM 1 TO 2J+1, 1 IS INDEX FOR MJ=-J AND 2J+1 IS INDEX
C      FOR MJ=J
C      SUBROUTINE THEORY (IQ,JQ,KQ,IOP)
C      DIMENSION OA(8,16,16),OB(8,16,16),OC(8,16,16),THETA(3,20),W(16)
C      DIMENSION CEF(16,16,2),GIVE(300),ANM(3,4,2),AJ(20),SIGN(2)
C      DIMENSION E(100),R(100),V(100),P(3,40),X(20),QSQ(3),DP(20),S(120)
C      DIMENSION DEF(16,16,2),W1(16)
C      DIMENSION HEAD(8,33),FMT(8,12),FMTA(12),EVECI(16),EVECR(16)
C      DIMENSION C(16,16)
C      DIMENSION NOBSVR(20,20),NORMAL(20),S1(120)
C      COMMON/COMTHE/NFORM,P
C      COMMON/COMQSQ/NE,E,S,R
C      COMMON/COMWAV/C1(256)
C      COMMON DUMMY(281), NP
C      COMPLEX C,CTEMP,C1
C      COMPLEX CSQRT,CONJG
C      CALL OVERFL(J123)
10  IF(NFORM)1,1,2
1  READ  (5,100)NTERM,NJ,XJ,IW,IDEG,DELTA,NRDM
100  FORMAT(2I2,F10.5,2I2/E20.5,I3)

```

```
NRDM=NRDM+1
DO 91 I=1,NRDM
91 IRDM=RDM(XRDM)
READ(5,73) SYMTRY,C3HSYM
73 FORMAT(12A6)
DO 999 M=1,NTerm
READ (5,101)(THETA(N,M),N=1,3),AJ(M)
101 FORMAT(3E20.5,F10.5)
READ(5,99) (NOBSVR(M,N), N=1,16),NORMAL(M)
99 FORMAT(16I1,12)
999 CONTINUE
DO 1000 I=1,8
DO 1000 J=1,16
DO 1000 K=1,16
OA(I,J,K)=0.
OB(I,J,K)=0.
OC(I,J,K)=0.
1000 CONTINUE
DO 998 K=1,NJ
READ(5,103) NOP,(HEAD(K,I),I=1,33),(FMT(K,J),J=1,12)
103 FORMAT(I2/20A4/13A4/12A6)
DO 997 L=1,NOP
READ(5,102) I,J,(OA(K,I,J)),I,J,(OB(K,I,J)),I,J,(OC(K,I,J))
102 FORMAT (2I2, E20.8)
997 CONTINUE
AK=K
LMAX=AK+XJ+0.52
DO 996 L=1,LMAX
MIN=L+1
JMAX=2.0*(AK+XJ)+1.01
MAX=JMAX+1-L
DO 996 N=MIN,MAX
NA=JMAX+1-N
OA(K,MAX,N)=OA(K,NA,L)
OB(K,MAX,N)=OB(K,NA,L)
OC(K,MAX,N)=OC(K,NA,L)
996 CONTINUE
DO 995 L=1,JMAX
DO 850 N=1,L
OA(K,N,L)=OA(K,L,N)
OB(K,N,L)=OB(K,L,N)
OC(K,N,L)=OC(K,L,N)
850 CONTINUE
995 CONTINUE
998 CONTINUE
C          SETTING UP OF ANM
DO 1001 I=1,3
DO 1001 J=1,4
DO 1001 K=1,2
ANM(I,J,K)=0.
1001 CONTINUE
```

```

2  IA=0
   IS=1
   ISA=1
   ICTR=0
   DO 994 N=1,3
   MAX=N+1
   DO 994 M=1,MAX
   DO 994 L=1,2
   IF(L-N) 111,111,994
111 CONTINUE
   IF(M-L)994,993,993
993 ICTR=ICTR+1
   IF(SYMTY.EQ.C3HSYM)
1  GO TO (5,994,5,994,994,994,994,5,994,994,994,5,994), ICTR
5  IA=IA+1
   IF(IA-IQ)992,991,992
992 ANM(N,M,L)=P(KQ,IA)
   GO TO 994
991 ANM(N,M,L)=P(JQ,IA)
994 CONTINUE
   IF(NFORM)112,113,112
113 WRITE(6,3000)((ANM(N,M,L), L=1,2), M=1,4), N=1,3)
3000 FORMAT(5HOANML/(6E20.8))
112 CONTINUE

```

C CALCULATE CEF MATRIX ELEMENTS

```

SIGN(1)=1.0
SIGN(2)=-1.0
DO 900 I=1,NTerm
IJ=AJ(I)-XJ+.01
JMAX=2.0*AJ(I)+1.01
IF(SYMTY.NE.C3HSYM) IA=NP-NTerm
IF(IQ.GT.IA+1) GO TO 52
DO 903 J=1,JMAX
DO 903 K=1,JMAX
DO 903 L=1,2
CEF(J,K,L)=0.0
903 CONTINUE
DO 901 J=1,JMAX
DO 901 K=1,J
IF(J-K)800,801,800
801 M=1
GO TO 810
800 IF(J-K-2)901,802,803
802 M=2
GO TO 810
803 IF(J-K-4)901,804,805
804 M=3
GO TO 810
805 IF(J-K-6)901,806,901
806 M=4
810 CONTINUE

```

```

      DO 899 L=1,2
      CEF(J,K,L)=SIGN(L)*(THETA(1,I)*OA(IJ,J,K)*ANM(1,M,L)+THETA(2,I)*
1      OB(IJ,J,K)*ANM(2,M,L)+THETA(3,I)*OC(IJ,J,K)*ANM(3,M,L))
      CEF(K,J,L)=SIGN(L)*CEF(J,K,L)
899 CONTINUE
901 CONTINUE
C      DIAGONALIZE THE HERMITIAN MATRIX CEF
      IF(IDEQ-2)500,501,500
501 JMAX=JMAX/IDEQ
      JAB=1
      DO 503 J=1,JMAX
      KAB=1
      DO 504 K=1,J
      DO 505 L=1,2
      DEF(J,K,L)=CEF(JAB,KAB,L)
      DEF(K,J,L)=SIGN(L)*DEF(J,K,L)
505 CONTINUE
      KAB=KAB+2
504 CONTINUE
      JAB=JAB+2
503 CONTINUE
      IF(JMAX.EQ.1) W(1)=DEF(1,1,1)
      IF(JMAX.EQ.1) GO TO 506
      IF(JMAX.NE.2) GO TO 499
      TEMP=SQRT((DEF(1,1,1)-DEF(2,2,1))**2+4.0*(DEF(2,1,1)**2+DEF(2,1,2)
1**2))
      W(1)=(DEF(1,1,1)+DEF(2,2,1)+TEMP)/2.0
      W(2)=(DEF(1,1,1)+DEF(2,2,1)-TEMP)/2.0
      GO TO 506
499 CALL EIGENH(DEF,W,JMAX,DELTA)
      GO TO 506
500 MZ=0
      DO 515 M=1,2
      JMAX1=(JMAX-1)/2
      IF(M.EQ.2) JMAX1=(JMAX+1)/2
      JZ=2
      IF(M.EQ.2) JZ=1
      DO 507 J=1,JMAX1
      KZ=2
      IF(M.EQ.2) KZ=1
      DO 508 K=1,J
      DO 509 L=1,2
      DEF(J,K,L)=CEF(JZ,KZ,L)
509 DEF(K,J,L)=SIGN(L)*DEF(J,K,L)
508 KZ=KZ+2
507 JZ=JZ+2
      IF(JMAX1.EQ.1) W1(1)=DEF(1,1,1)
      IF(JMAX1.EQ.1) GO TO 511
      IF(JMAX1.NE.2) GO TO 512
      TEMP=SQRT((DEF(1,1,1)-DEF(2,2,1))**2+4.0*(DEF(2,1,1)**2+DEF(2,1,2)
1**2))

```

```

W1(1)=(DEF(1,1,1)+DEF(2,2,1)+TEMP)/2.0
W1(2)=(DEF(1,1,1)+DEF(2,2,1)-TEMP)/2.0
GO TO 511
512 CALL EIGENH(DEF,W1,JMAX1,DELTA)
511 DO 510 J=1,JMAX1
    MZ=MZ+1
510 W(MZ)=W1(J)
515 CONTINUE
506 KMAX=JMAX-1
    DO 17 K=1,KMAX
        KP1=K+1
        DO 17 J=KP1,JMAX
            IF(W(K)-W(J))17,17,18
18 TEMP=W(K)
        W(K)=W(J)
        W(J)=TEMP
17 CONTINUE
    INORM=NORMAL(I)
    TEMP=W(INORM)
    DO 69 K=1,JMAX
69 W(K)=W(K)-TEMP
    DO 50 K=1,JMAX
        IF(NOBSVR(I,K).EQ.1) GO TO 50
        S(IS)=W(K)
        S1(IS)=S(IS)
        IS=IS+1
50 CONTINUE
    GO TO 53
52 IF(IDEQ.EQ.2) JMAX=JMAX/2
53 IZS=KQ
    IZT=IA+I
    IF(IQ.EQ.IZT) IZS=JQ
    DO 51 K=1,JMAX
        IF(NOBSVR(I,K).EQ.1) GO TO 51
        S(ISA)=S1(ISA)+P(IZS,IZT)
        ISA=ISA+1
51 CONTINUE
    IF(IOP.NE.0) GO TO 900
    IF(IDEQ.EQ.2) JMAX=2*JMAX
    CALL EIGENH(CEF,W,JMAX,DELTA)
    DO 6005 J=1,JMAX
        DO 6005 K=1,JMAX
            INDEX=J+K*JMAX-JMAX
6005 C(K,J)=C1(INDEX)
6006 KMAX=JMAX-1
C    MULTIPLY C BY PROPER PHASE FACTOR
    DO 4000 J=1,JMAX
        TEMP=REAL(C(1,J))
        IF(TEMP.EQ.0.0) GO TO 4001
        CTEMP=CSQRT(CONJG(C(JMAX,J))/C(1,J))
        GO TO 4002

```

```
4001 CTEMP=CSQRT(-CONJG(C(KMAX,J))/C(2,J))
4002 DO 4003 K=1,JMAX
4003 C(K,J)=CTEMP*C(K,J)
4000 CONTINUE
      DO 6017 K=1,KMAX
      KP1=K+1
      DO 6017 J=KP1,JMAX
      IF(W(K).LE.W(J)) GO TO 6017
      TEMP=W(K)
      W(K)=W(J)
      W(J)=TEMP
      DO 6018 L=1,JMAX
      CTEMP=C(L,K)
      C(L,K)=C(L,J)
6018 C(L,J)=CTEMP
6017 CONTINUE
      WRITE(6,6000)(HEAD(IJ,K),K=1,33)
6000 FORMAT(33A4)
      DO 6001 K=1,12
6001 FMTA(K)=FMT(IJ,K)
      DO 6002 J=1,JMAX
      DO 6003 K=1,JMAX
      EVECR(K)=REAL(C(K,J))
6003 EVECI(K)=AIMAG(C(K,J))
6002 WRITE(6,FMTA) W(J),(EVECR(K),K=1,JMAX),(EVECI(K),K=1,JMAX)
900 CONTINUE
      RETURN
      END
```

```
C      QSQUAR...
C      FUNCTION TO CALCULATE VALUE OF Q**2, WHERE CHI**2 IS MINIMUM VALUE
C      OF THIS FUNCTION
      FUNCTION QSQUAR(IQ,JQ,KQ)
      DIMENSION E(100),R(100),V(100),P(3,20),X(20),QSQ(3),DP(20),S(1500)
      DIMENSION GIVE(300)
      COMMON GIVE,S,E,R,V,P,X,QSQ,NE,NP,IQ,JQ,KQ,IOP,XTEST
      QSQUAR = 0.0
      CALL THEORY(IQ,JQ,KQ,1)
      DO 10 L=1,NE
10  QSQUAR=QSQUAR+((E(L)-S(L))/R(L))**2
      RETURN
      END
```

```
C      LEIGEN...
C      THIS IS A LINK BETWEEN A PROGRAM CALLING EIGENH AND HERM.
      SUBROUTINE EIGENH(CEF,W,JMAX,DELTA)
      COMMON/COMHER/B(16),H(200)
      COMMON/COMWAV/C
      COMPLEX H,C,CMPLX
      DIMENSION C(16,16),CEF(16,16,2),W(16)
      IBEGIN=16-JMAX
      DO 1 I=1,JMAX
      IS=I+IBEGIN
1      B(IS)=CEF(I,I,1)
      I=1
      IMAX=JMAX-1
      DO 2 J=1,IMAX
      JP1=J+1
      DO 2 K=JP1,JMAX
      H(I)=CMPLX(CEF(J,K,1),CEF(J,K,2))
2      I=I+1
      KZE=I+I/2-1
      H(KZE)=(0.0,0.0)
      H(KZE+1)=(0.0,0.0)
      CALL HERM(H,JMAX,C,0,DELTA,IT)
      DO 3 I=1,JMAX
      IS=I+IBEGIN
3      W(I)=B(IS)
      RETURN
      END
```

* HERM...
* THIS SUBROUTINE DIAGONALIZES A HERMITIAN MATRIX AND OBTAINS ALL
* EIGENVALUES AND EIGENVECTORS. IT IS SHARE NO. 884 PK HMEE WHICH
* HAS BEEN MODIFIED SO THAT IT MAY BE CALLED FROM A FORTRAN PROGRAM
* ONLY THE MODIFICATIONS ARE SHOWN HERE.
* THE CALL STATEMENT TO BE USED IS CALL HERM(H,N,U,PR,DELTA,IT)
* ALL ARGUMENTS HAVE SAME MEANING AS DESCRIBED IN SHARE NO. 884
* WRITE UP, PR SHOULD ALWAYS BE ZERO AND IT IS THE NUMBER OF
* ITERATIONS

HERM SAVE 1,2
SXA XR4,4
CAL 3,4
STA H1
CAL* 4,4
LGL 18
STD H1
CAL 5,4
STA H2
CAL* 6,4
LGL 18
STD H2
CAL* 7,4
SLW H3
TSX HMEE,4
H1 PZE **,**
H2 PZE **,**
H3 BSS 1
XR4 AXT **,4
CAL COMMON+20
SLW* 8,4
RETURN HERM

* FIRST CARD OF SHARE NO. 884 FOLLOWS THIS CARD

* LAST CARD OF SHARE NO. 884 PRECEDES THIS CARD
COMMON BSS 23
END

ICARME

The required card decks are:

1. ICA
2. RME
3. SIXJ
4. DELTA
5. FACT

The programs in decks 3 and 4 were written by B.A. Zimmerman.
The listings of decks 1-5 follow.

```

C      I C A ...
C      THIS IS A PROGRAM TO CALCULATE THE OPERATOR EQUIVALENT FACTORS
C      IN THE INTERMEDIATE COUPLING APPROXIMATION
C      FOR TM IV OR PR IV GIVEN THE SLATER INTEGRALS, SPIN-ORBIT
C      COUPLING PARAMETER, AND PURE L-S OE FACTORS.
C      REF. F.H. SPEDDING, PHY.REV. 58,255(1940) AND GRUBER AND CONWAY
C      J. CHEM. PHY. 32, 1178(1960).
C      INPUT DATA
C      E1, E2, E3=RACAH'S LINEAR COMBINATION OF SLATER INTEGRALS
C      F2, F4, F6
C      ZETA1=SPIN-ORBIT COUPLING PARAMETER
      DIMENSION AS(3),AL(3)
      DIMENSION S(3,3), EV(3,3), E(3)
      DIMENSION ERASS (20),A(3),B(3),G(3),AE(3),BE(3),GE(3)
1    READ(5,100) E1,E2,E3,ZETA1
100  FORMAT ( F20.5)
      F2=(E1+143.0*E2+11.0*E3)/42.0
      F4=(6.0*F2-39.0*E2-E3)/11.0
      F6=(7.0*F2-18.0*E2-3.0*E3)/77.0
      ZETA=-ZETA1/2.0
      WRITE(6,1000) E1,E2,E3,ZETA1,F2,F4,F6,ZETA
1000 FORMAT(4H1E1=1PE14.7,5X3HE2=E14.7,5X3HE3=E14.7,5X6HZETA'=E14.7/
14HOF2=E14.7,5X3HF4=E14.7,5X3HF6=E14.7,5X5HZETA=E14.7)
C      PURE ELECTROSTATIC ENERGY LEVELS
      E3H = 0.0
      E3F = 15.0 * F2 + 18.0 * F4 - 273.0 * F6
      E1G = - 5.0 * F2 + 148.0 * F4 + 91.0 * F6
      E1D = 44.0 * F2 - 48.0 * F4 + 728.0 * F6
      E1I = 50.0 * F2 + 60.0 * F4 + 14.0 * F6
      E3P = 70.0 * F2 + 84.0 * F4 - 1274.0 * F6
      E1S = 85.0 * F2 + 249.0 * F4 + 1729.0 * F6
C      COULOMBIC AND SPIN-ORBIT MATRICES, CHARACTERIZED BY J
      S(1,1) = E3F + 4.0 * ZETA
      S(2,2) = E1D
      S(3,3) = E3P - ZETA
      S(2,1) = 2.0 * 2.449490 * ZETA
      S(3,1) = 0.0
      S(3,2) = - 3.0 * 1.414214 * ZETA
      DO 2 I = 2, 3
      DO 2 J = 1, 2
2    S(J,I) = S(I,J)
      AS(1)=1.0
      AS(2)=0.0
      AS(3)=1.0
      AL(1)=3.0
      AL(2)=2.0
      AL(3)=1.0
      AJ=2.0
      NORDER = 3
      IFLAG = 1
      WRITE (6,400)

```

```

400 FORMAT ( 1H1 12X 6HENERGY 15X 3H3F2 15X 3H1D2 15X 3H3P2 13X
15HALPHA 14X 4HBETA 13X 5HGAMMA )
GO TO 30
10 S(1,1) = E3H + 6.0 * ZETA
S(2,2) = E1G
S(3,3) = E3F - 3.0 * ZETA
S(2,1) = 2.0 * 3.162278 / 1.732051 * ZETA
S(3,1) = 0.0
S(3,2) = - 2.0 * 3.316625 / 1.732051 * ZETA
S(1,2) = S(2,1)
S(1,3) = 0.0
S(2,3) = S(3,2)
AL(1)=5.0
AL(2)=4.0
AL(3)=3.0
AJ=4.0
NORDER = 3
IFLAG = 2
WRITE (6,500)
500 FORMAT (1H0 12X6HENERGY 15X 3H3H4 15X3H1G4 15X 3H3F4 13X
15HALPHA 14X 4HBETA 13X 5HGAMMA )
GO TO 30
20 S(1,1) = E1I
S(2,2) = E3H - 5.0 * ZETA
S(2,1) = - 2.449490 * ZETA
S(1,2) = S(2,1)
AS(1)=0.0
AS(2)=1.0
AL(1)=6.0
AL(2)=5.0
AJ=6.0
NORDER = 2
IFLAG = 3
WRITE (6,600)
600 FORMAT (1H0 12X 6HENERGY 15X 3H1I6 15X 3H3H6 13X
15HALPHA 14X 4HBETA 13X 5HGAMMA )
TEMP=SQRT((S(1,1)+S(2,2))**2+4.0*(S(1,2))**2-4.0*S(1,1)*S(2,2))
E(1)=(S(1,1)+S(2,2)+TEMP)/2.0
E(2)=(S(1,1)+S(2,2)-TEMP)/2.0
DO 12 I=1,2
TEMP=(E(I)-S(1,1))/S(1,2)
EV(1,I)=1.0/SQRT(1.0+TEMP**2)
12 EV(2,I)=TEMP/SQRT(1.0+TEMP**2)
GO TO 31
30 CALL EIGVV(S,EV,E,NORDER,ERASS)
31 DO 25 I=1,NORDER
A(I)=RME(AS(I),AL(I),AL(I),AJ,AJ,2.0)
B(I)=RME(AS(I),AL(I),AL(I),AJ,AJ,4.0)
25 G(I)=RME(AS(I),AL(I),AL(I),AJ,AJ,6.0)
IF(NORDER.EQ.2) GO TO 5
A13=RME(AS(1),AL(1),AL(3),AJ,AJ,2.0)

```

```
B13=RME(AS(1),AL(1),AL(3),AJ,AJ,4.0)
G13=RME(AS(1),AL(1),AL(3),AJ,AJ,6.0)
5 CONTINUE
WRITE(6,300)(A(I),B(I),G(I), I=1,NORDER),A13,B13,G13
300 FORMAT(E20.8)
DO 3 I = 1, NORDER
  AE(I) = 0.0
  BE(I) = 0.0
  GE(I) = 0.0
  DO 4 J = 1, NORDER
    AE(I) = AE(I) + A(J) * (EV(J,I))**2
    BE(I) = BE(I) + B(J) * (EV(J,I))**2
  4 GE(I) = GE(I) + G(J) * (EV(J,I))**2
  IF(NORDER.EQ.2) GO TO 3
  AE(I) = AE(I) + A13 * EV(1,I) * EV(3,I)*2.0
  BE(I) = BE(I) + B13 * EV(1,I) * EV(3,I)*2.0
  GE(I) = GE(I) + G13 * EV(1,I) * EV(3,I)*2.0
3 CONTINUE
IF(NORDER.EQ.2) GO TO 63
WRITE (6,200)(E(I), (EV(J,I),J = 1,NORDER), AE(I), BE(I), GE(I),
1 I = 1,NORDER)
200 FORMAT (1H01P7E18.7)
GO TO (10,20), IFLAG
63 WRITE (6,201)(E(I), (EV(J,I),J = 1,NORDER), AE(I), BE(I), GE(I),
1 I = 1,NORDER)
201 FORMAT (1H01P6E18.7)
GO TO 1
STOP
END
```

```

C      R M E ...
C      THIS IS A FUNCTION TO CALCULATE THE REDUCED MATRIX ELEMENTS OR
C      OPERATOR EQUIVALENT FACTORS FOR THE 4F12 ELECTRON CONFIGURATION.
C      THE ELEMENTS ARE OF THE FORM (S,L,J 11N11 S,L',J').
C      REF. B.R.JUDD, PROC. ROY. SOC. A241,414(1957).
C      THIS VERSION IS FOR J=J'.
      FUNCTION RME(AS,AL,BL,AJ,BJ,AN)
      TEMPJ=SQRT((2.0*AJ+1.0)*(2.0*BJ+1.0))
      TEMPL=SQRT((2.0*AL+1.0)*(2.0*BL+1.0))
      L1=AL
      L2=BL
      J1=AJ
      J2=BJ
      IS=AS
      W1=SIXJ(AL,AJ,BL,BJ,AS,AN)*(-1.0)**(L1+L2+J1+J2)
      W2=SIXJ(3.0,AL,3.0,BL,3.0,AN)*(-1.0)**(L1+L2+J1+J2)
      N=AN
      J=AJ
      SFACT=SQRT(FACT(2*J-N)/FACT(2*J+N+1))
      RME1=(-1.0)**(IS- J+2 )*TEMPJ*TEMPL*SFACT*W1*W2
      GO TO (1,2,1,4,1,6),N
2     RME=16.0*SQRT(7.0/15.0)*RME1
      RETURN
4     RME=-32.0*SQRT(14.0/11.0)*RME1
      RETURN
6     RME=1280.0*SQRT(7.0/429.0)*RME1
      RETURN
1    WRITE(6,100)
100  FORMAT(32HORME DOES NOT EXIST FOR THIS N )
      STOP
      END

```

```
C      SIXJ...
C      A FUNCTION FOR SIX J SYMBOLS          2/25/64
C      ROTENBERG ET. AL. PAGE 13 EQUATION (2.3)
C      INPUT SIXJ(J1,J2,L2,L1,J3,L3) IN FLOATING POINT
C      REQUIRES DELTA AND FACTORIAL ROUTINES
      FUNCTION SIXJ(A,B,C,D,E,F)
      TRI1 = A+B-E
      IF(TRI1)2,1,1
2      SIXJ = 0.0
      RETURN
1      TRI1 = A-B+E
      IF(TRI1)2,3,3
3      TRI1 = -A+B+E
      IF(TRI1)2,4,4
C      FIRST TRIANGULAR TEST COMPLETED
4      TRI2 = D+C-E
      IF(TRI2)2,5,5
5      TRI2 = D-C+E
      IF(TRI2)2,6,6
6      TRI2 = -D+C+E
      IF(TRI2)2,7,7
C      SECOND TRIANGULAR TEST COMPLETED
7      TRI3 = A+C-F
      IF(TRI3)2,8,8
8      TRI3=A-C+F
      IF(TRI3)2,9,9
9      TRI3 = -A+C+F
      IF(TRI3)2,10,10
C      THIRD TRIANGULAR TEST COMPLETED
10     TRI4 = D+B-F
      IF(TRI4)2,11,11
11     TRI4 = D-B+F
      IF(TRI4)2,12,12
12     TRI4=-D+B+F
      IF(TRI4)2,13,13
C      FOURTH TRIANGULAR TEST COMPLETED
13     DEL1 = DELTA(A,B,E)
      DEL2 = DELTA(D,C,E)
      DEL3 = DELTA(D,B,F)
      DEL4 = DELTA(A,C,F)
      DELX = DEL1*DEL2*DEL3*DEL4
      N = A+B+C+D
      PHZ = (-1.0)**N
      SUM = 0.0
      AK = 0.0
24     S1 = A+B-E-AK
      IF(S1)22,16,16
16     M = S1
      FS1 = FACT(M)
      S2 = C+D-E-AK
      IF(S2)22,18,18
```

```
18  M = S2
    FS2 = FACT(M)
    S3 = A+C-F-AK
    IF(S3)22,19,19
19  M = S3
    FS3 = FACT(M)
    S4 = D+B-F-AK
    IF(S4)22,20,20
20  M = S4
    FS4 = FACT(M)
    S5 = -A-D+E+F+AK
    IF(S5)17,21,21
21  M = S5
    FS5 = FACT(M)
    S6 = -B-C+E+F+AK
    IF(S6)17,23,23
23  M = S6
    FS6 = FACT(M)
    N = AK
    SPHZ = (-1.0)**N
    TOP = A+B+C+D+1.0-AK
    M = TOP
    FTOP = FACT(M)
    TOP = SPHZ*FTOP
    M = AK
    FAK = FACT(M)
    DENOM = FAK*FS1*FS2*FS3*FS4*FS5*FS6
    SUM = SUM + (TOP/DENOM)
17  AK = AK + 1.0
    GO TO 24
22  SIXJ = PHZ*DELX*SUM
    RETURN
    END
```

```
C      DELTA...
C      FUNCTION DELTA(A,B,C)
C      ROTENBERG ET. AL. PAGE 13 (2.4)
      FUNCTION DELTA(A,B,C)
      S1 = A + B - C
      M = S1
      FS1 = FACT(M)
      S2 = A + C - B
      M = S2
      FS2 = FACT(M)
      S3 = B + C - A
      M = S3
      FS3 = FACT(M)
      DENOM = A+B+C+1.0
      M = DENOM
      FD = FACT(M)
      DELTA = SQRT((FS1*FS2*FS3)/FD)
      RETURN
      END
```

```
C      FACT...  
C      CALCULATES N FACTORIAL  
      FUNCTION FACT(N)  
      A=N  
      FACT=0.0  
      IF(A.LT.0.0) RETURN  
      FACT=1.0  
      IF(A.EQ.0.0) RETURN  
      FACT=FACT*A  
      DO 1 I=1,100  
      B=I  
      C=A-B  
      IF(C.EQ.0.0) RETURN  
      FACT=FACT*C  
1     CONTINUE  
      WRITE(6,100)  
100  FORMAT(19H0FACTORIAL OVERFLOW  )  
      STOP  
      END
```

QTAVE

The required card decks are:

1. SEARCH
2. COREL
3. OUTPUT
4. DERIV 3
5. JPLOT
6. CEFMAT
7. THEORY 6
8. QSQUAR see listings for OPTIC
9. HERM see SHARE no. 884

The listings of decks 1-7 follow.

```

C SEARCH...
C THIS PROGRAM USES THE METHOD OF DIRECT SEARCH TO OBTAIN BEST
C VALUE OF CHI**2
C INPUT DATA
C NE=NO. OF ENERGY LEVELS MEASURED
C NP=NO. OF SHIELDING PARAMETERS
C NPP=NO. OF SHIELDING PARAMETERS WITH NON-ZERO STEP SIZE
C ITIME= MAX. XEQ TIME ALLOWED
C E(I)=MEASURED ENERGY LEVELS
C R(I)=ERROR IN MEASURED ENERGY LEVELS
C V(I)=LEVEL IDENTIFICATION
C P(2,I)=INITIAL VALUE OF PARAMETERS
C X(I)=STEP SIZE FOR EACH PARAMETER FOR INITIAL CYCLE
C XMIN=2**N , WHERE N IS MAX NO. OF CYCLES ALLOWED I.E. FINAL
C STEP SIZE WILL BE X(I)/2**N
C DIMENSION E(100),R(100),V(100),P(3,20),X(20),QSQ(3),DP(20),S(1500)
C DIMENSION AB(20)
C DIMENSION GIVE(300)
C COMMON GIVE,S,E,R,V,P,X,QSQ,NE,NP,IQ,JQ,KQ,IOP,XTEST,NFORM,NMOVE,A
C COMMON /COMTIM/ITIME
C READ (5,99)NE,NP,NPP,ITIME
99 FORMAT(I3/I3/I3/I6)
C CALL ICLOCK(NTIME)
C ITIME=NTIME+ITIME
C READ (5,800)(E(I),R(I),V(I), I=1,NE)
800 FORMAT(3F20.5)
C READ (5,500)AA,BB,(AB(I), I=1,NP)
500 FORMAT(12A6)
C NFORM=0
1000 READ (5,200)(P(2,I),X(I), I=1,NP)
200 FORMAT(2F20.5)
C READ (5,300)XMIN
300 FORMAT(F20.5)
C NMOVE=0
C QSQ(2)=QSQUAR(1,2,2)
C NFORM=1
C A=NE-NPP
C CHI=QSQ(2)/A
C WRITE (6,700)(AB(I),I=1,NP)
700 FORMAT(1H1,(10X,A6,14X,A6,14X,A6,14X,A6,14X,A6,14X,A6))
C WRITE (6,701)
701 FORMAT(9X,7H CHI**2//29H INITIAL VALUES OF PARAMETERS)
C WRITE (6,702)(P(2,I),I=1,NP)
702 FORMAT(6E20.8)
C WRITE (6,703)CHI,(X(I),I=1,NP)
703 FORMAT(1PE20.7//24H INITIAL VALUES OF STEPS/(0P6E20.8))
C FORMING PATTERN
C XTEST=1.0
13 NZERO=0
C NFORM=NFORM+1
C DO 2 I=1,NP

```

```

      IF(X(I))50,5,50
50 CONTINUE
      P(1,I)=P(2,I)-X(I)
      QSQ(1)=QSQUAR(I,1,2)
      P(3,I)=P(2,I)+X(I)
      QSQ(3)=QSQUAR(I,3,2)
      IF(QSQ(2)-QSQ(1))3,3,4
3 IF(QSQ(2)-QSQ(3))5,5,6
4 DP(I)=-1.0
      QSQ(2)=QSQ(1)
      GO TO 7
5 DP(I)=0.0
      NZERO=NZERO+1
      GO TO 7
6 DP(I)=+1.0
      QSQ(2)=QSQ(3)
7 P(2,I)=P(2,I)+DP(I)*X(I)
2 CONTINUE
C      CHECK TO SEE IF PATTERN IS NON-ZERO
      IF(NZERO-NP)8,9,8
9 XTEST=2.0*XTEST
      CALL ICLOCK(LPTIME)
      IF(LPTIME.GT.ETIME) GO TO 11
20 IF(XTEST-XMIN)10,10,11
11 CALL OUTPUT
      GO TO 1000
10 DO 12 I=1,NP
12 X(I)=X(I)/2.0
      CHI=QSQ(2)/A
      WRITE          (6,100)(P(2,I),I=1,NP)
100 FORMAT(6E20.8)
      WRITE          (6,101)CHI,NFORM,NMOVE,XTEST
101 FORMAT(1PE20.7/15X,7H NFORM= I6,7X,7H NMOVE= I6,7H XTEST= OPF9.1/)
      GO TO 13
C      MAKE PATTERN MOVES
8 NMOVE=0
18 NMOVE=NMOVE+1
      DO 14 I=1,NP
14 P(1,I)=P(2,I)+DP(I)*X(I)
      QSQ(1)=QSQUAR(1,1,1)
      IF(QSQ(2)-QSQ(1))13,13,15
15 QSQ(2)=QSQ(1)
      DO 16 I=1,NP
16 P(2,I)=P(1,I)
      CALL ICLOCK(LPTIME)
      IF(LPTIME.GT.ETIME) GO TO 11
17 GO TO 18
      END

```

```
C      COREL...
C      THIS SUBROUTINE CALCULATES THE CORRELATION MATRIX FOR A LEAST
C      SQUARE ANALYSIS.
      SUBROUTINE COREL
      DIMENSION A(5,5),DER(5,20),AINV( 50,5),B(50,1)
      DIMENSION E(100),R(100),V(100),P(3,20),X(20),QSQ(3),DP(20),S(1500)
      DIMENSION GIVE(300)
      COMMON GIVE,S,E,R,V,P,X,QSQ,NE,NP,IQ,JQ,KQ,IOP,XTEST,NFORM,NMOVE
      COMMON /COMTIM/ITIME
      NK=NE
      DO 5 I=1,NP
      DO 5 K=1,NK
      NE=K
      CALL ICLOCK(LPTIME)
      IF(LPTIME.GT.ITIME) GO TO 90
5     DER(I,K)=DERIV(I,K)
      DO 10 I=1,NP
      DO 10 J=1,I
      AINV(I,J)=0.0
      DO 10 K=1,NK
      AINV(I,J)=AINV(I,J)+DER(I,K)*DER(J,K)/(R(K)*R(K))
10    CONTINUE
      NPM1=NP-1
      DO 11 I=1,NPM1
      IP1=I+1
      DO 11 J=IP1,NP
      AINV(I,J)=AINV(J,I)
11    CONTINUE
      WRITE(6,200)((AINV(I,J), I=1,NP), J=1,NP)
200   FORMAT(36H  INVERSE OF BEST CORRELATION MATRIX//(5E20.8))
      CALL MATINV(AINV,NP,B,0,DETERM)
      DO 12 I=1,NP
      DO 12 J=1,NP
      A(I,J)=SQRT(AINV(I,J))
12    CONTINUE
      WRITE (6,100)((A(I,J), I=1,NP), J=1,NP)
100   FORMAT(44H  BEST CORRELATION MATRIX (SQRT OF ELEMENTS)//(5E20.8))
      90 RETURN
      END
```

```
C      OUTPUT...
C      THIS SUBROUTINE CONTROLS THE OUTPUT PHASE OF SEARCH
      SUBROUTINE OUTPUT
      DIMENSION E(100),R(100),V(100),P(3,20),X(20),QSQ(3),DP(20),S(1500)
      DIMENSION GIVE(300)
      COMMON GIVE,S,E,R,V,P,X,QSQ,NE,NP,IQ,JQ,KQ,IOP,XTEST,NFORM,NMOVE,A
      CHI=QSQ(2)/A
      XTEST=XTEST/2.0
      WRITE (6,200)
200  FORMAT(38H FINAL VALUES OF PARAMETERS AND CHI**2)
      WRITE (6,800)(P(2,I),I=1,NP)
800  FORMAT(6E20.8)
      WRITE (6,801)CHI,NFORM,NMOVE,XTEST
801  FORMAT(1PE20.7/15X,7H NFORM= I6,7X,7H NMOVE= I6,7H XTEST= OPF9.1/)
      WRITE (6,300)(X(I), I=1,NP)
300  FORMAT(22H FINAL VALUES OF STEPS/(6E20.8))
      CALL COREL
      CALL THEORY(1,2,2,0)
      RETURN
      END
```

```
C      D E R I V 3 .....
C      THIS FUNCTION CALCULATES THE PARTIAL DERIVATIVE OF THE OUTPUT
C      OF THE SUBROUTINE THEORY WITH RESPECT TO THE PARAMETER IP AT THE
C      POINT JP.
C      DERIV3 IS FOR THE SPECIAL CASE OF THE SHIELDING PARAMETERS
C      ONLY IN THE CASE OF C2 SYMMETRY.
      FUNCTION DERIV(IP,JP)
      COMMON/COMDER/DR(300),DS(300)
      IF(IP-1)10,10,20
10  DERIV=DR(JP)
      GO TO 30
20  DERIV=DS(JP)
30  RETURN
      END
```

```

C      JPLOT...
C JPLOT, THIS SUBROUTINE PLOTS A SINGLE VALUED FUNCTION
C ON THE OFF-LINE PRINTER. THE ORDINATES ARE PLOTTED ACROSS THE PAGE
C AND THE ABSCISSAS ARE PLOTTED DOWN THE PAGE
C      S= ARRAY TO BE PLOTTED (ONE DIMENSIONAL)
C      NP= NO. OF ELEMENTS IN S
C      NL= NO. OF LINES THAT PLOT IS TO COVER
C      X0= LOWER LIMIT OF ORDINATES
C      X1= UPPER LIMIT OF ORDINATES
C      X= UNITS PER LINE (SCALE FACTOR)
C      DD= AN ALPHAMERIC TITLE FOR PLOT, 10A6
C      LAB= NO. OF THE PLOT, MUST START WITH 1
C      WHEN LAB=1 THE PLOT SYMBOLS ARE READ. THE PLOT SYMBOLS, AA(I),
C      CONSIST OF 7 WORDS THAT CONTAIN 6 BLANKS OR 5 BLANKS AND ONE
C      PLUS SIGN.
C      SUBROUTINE JPLOT(S,NP,NL,X0,X1,X,XI,DD,LAB)
C      DIMENSION S(1500),GIVE(300),AA(9),AB(20),DD(10)
C      COMMON GIVE , S
C      IF(LAB-1)1000,1000,1001
1000 READ (5,999)(AA(I), I=1,9)
999 FORMAT(9A6)
1001 JD=NP/NL
      X2=(X1+X0)/2.0
      WRITE (6,980)DD,X0,X2,X1
980 FORMAT(18H1 RESULTS OF JPLOT//10A6//12X,F7.2,43X,F7.2,43X,F7.2/
115X,102H *IIIIIIII*IIIIIIII*IIIIIIII*IIIIIIII*IIIIIIII*IIIIII
2III*IIIIIIII*IIIIIIII*IIIIIIII*IIIIIIII*)
      DO 998 J=1,NP,JD
      ABC=X*FLOAT(J)+XI
      DO 994 I=1,17
994 AB(I)=AA(7)
      IF(S(J)-X0)43,44,44
43 AB(1)=AA(8)
      AB(2)=AA(9)
      GO TO 990
44 IF(S(J)-X1)46,46,45
45 AB(16)=AA(8)
      AB(17)=AA(9)
      GO TO 990
46 PS=100.0*(S(J)-X0)/(X1-X0)+0.5
      IPS=PS
      ITEST=0
      DO 997 I=1,17
      IF(IPS-ITEST)952,995,952
952 IF(IPS-6-ITEST)950,991,991
991 ITEST=ITEST+6
997 CONTINUE
950 IDEL=IPS-ITEST
      GO TO (1,2,3,4,5),IDEL
995 AB(I)=AA(1)
      GO TO 990

```

```
4 AB(I)=AA(5)
  GO TO 990
3 AB(I)=AA(4)
  GO TO 990
2 AB(I)=AA(3)
  GO TO 990
1 AB(I)=AA(2)
  GO TO 990
5 AB(I)=AA(6)
990 WRITE (6,989)ABC,(AB(K),K=1,17)
989 FORMAT(7X,F6.1,3H I 17A6)
998 CONTINUE
  RETURN
  END
```

```

C      C E F M A T .....
C      THIS SUBROUTINE CALCULATES THE CEF MATRIX ELEMENTS OF A RARE
C      EARTH ION IN NTERM TERMS OF THE OPTICAL SPECTRA.  THE MAX J=15/2.
C      HIGHER J MAY BE HANDLED IF THE APPROPRIATE DIMENSION STATEMENTS
C      ARE CHANGED.  THE ELEMENTS ARE CALCULATED FROM GIVEN CEF PARAMET.
C      INPUT DATA
C      P(2,I)=CEF PARAMETERS IN THE FOLLOWING ORDER C20,C22,C40,C42,
C      C4-2,C44,C4-4,C60,C62,C6-2,C64,C6-4,C66,C6-6
C      NTERM=NO. OF OPTICAL LSJ TERMS
C      NJ=NO. OF DIFFERENT J VALUES IN TERMS
C      XJ=MIN. J VALUE - 1.0
C      IW=DUMMY VARIABLE
C      IDEG=1 FOR INTEGRAL J, 2 FOR HALF INTEGRAL J
C      THETA(N,M)=REDUCED MATRIX ELEMENTS, N IS ORDER,M IS TERM
C      IDENTIFICATION
C      AJ(I)=J VALUE FOR THE ITH TERM
C      NOP=NO. OF CARDS WITH OPERATOR EQUIVALENT MATRIX ELEMENTS FOR
C      EACH J VALUE DIVIDED BY 3
C      OA, OB, OC(K,I,J)=IJ OPERATOR EQUIVALENT MATRIX ELEMENT FOR
C      KTH J VALUE FOR ALPHA, BETA, GAMMA RESPECTIVELY, I AND J
C      GO FROM 1 TO 2J+1, 1 IS INDEX FOR MJ=-J AND 2J+1 IS INDEX
C      FOR MJ=J
C      SUBROUTINE CEFMAT(IQ,JQ,KQ)
C      DIMENSION OA(8,16,16),OB(8,16,16),OC(8,16,16),THETA(3,20)
C      DIMENSION P(3,20),          ANM(3,4,2),AJ(20),SIGN(2)
C      COMMON/COMTH/CEF(13,13,2)
C      READ(5,699)(P(2,I), I=1,14)
699  FORMAT(6E12.5)
C      1 READ (5,100)NTERM,NJ,XJ,IW,IDEG
100  FORMAT(2I2,F10.5,2I2)
C      DO 999 M=1,NTERM
C      READ (5,101)(THETA(N,M),N=1,3),AJ(M)
101  FORMAT(3E20.5,F10.5)
999  CONTINUE
C      DO 1000 I=1,8
C      DO 1000 J=1,16
C      DO 1000 K=1,16
C      OA(I,J,K)=0.
C      OB(I,J,K)=0.
C      OC(I,J,K)=0.
1000 CONTINUE
C      DO 998 K=1,NJ
C      READ (5,103)NOP
103  FORMAT (I2)
C      DO 997 L=1,NOP
C      READ (5,102)I,J,(OA(K,I,J),OB(K,I,J),OC(K,I,J))
102  FORMAT (2I2,3F20.5)
997  CONTINUE
C      AK=K
C      LMAX=AK+XJ+0.52
C      DO 996 L=1,LMAX

```

```
MIN=L+1
JMAX=2.0*(AK+XJ)+1.01
MAX=JMAX+1-L
DO 996 N=MIN,MAX
NA=JMAX+1-N
OA(K,MAX,N)=OA(K,NA,L)
OB(K,MAX,N)=OB(K,NA,L)
OC(K,MAX,N)=OC(K,NA,L)
996 CONTINUE
DO 995 L=1,JMAX
DO 995 N=1,L
OA(K,N,L)=OA(K,L,N)
OB(K,N,L)=OB(K,L,N)
OC(K,N,L)=OC(K,L,N)
995 CONTINUE
998 CONTINUE
C      SETTING UP OF ANM
DO 1001 I=1,3
DO 1001 J=1,4
DO 1001 K=1,2
ANM(I,J,K)=0.
1001 CONTINUE
2  IA=0
IS=1
DO 994 N=1,3
MAX=N+1
DO 994 M=1,MAX
DO 994 L=1,2
IF(L-N) 111,111,994
111 CONTINUE
IF(M-L)994,993,993
993 IA=IA+1
IF(IA-IQ)992,991,992
992 ANM(N,M,L)=P(KQ,IA)
GO TO 994
991 ANM(N,M,L)=P(JQ,IA)
994 CONTINUE
C      CALCULATE CEF MATRIX ELEMENTS
SIGN(1)=1.0
SIGN(2)=-1.0
I=1
IJ=AJ(I)-XJ+.01
JMAX=2.0*AJ(I)+1.01
DO 903 J=1,JMAX
DO 903 K=1,JMAX
DO 903 L=1,2
CEF(J,K,L)=0.0
903 CONTINUE
DO 901 J=1,JMAX
DO 901 K=1,J
IF(J-K)800,801,800
```

```
801 M=1
    GO TO 810
800 IF(J-K-2)901,802,803
802 M=2
    GO TO 810
803 IF(J-K-4)901,804,805
804 M=3
    GO TO 810
805 IF(J-K-6)901,806,901
806 M=4
810 CONTINUE
    DO 899 L=1,2
        CEF(J,K,L)=SIGN(L)*{THETA(1,I)*OA(IJ,J,K)*ANM(1,M,L)+THETA(2,I)*
1      OB(IJ,J,K)*ANM(2,M,L)+THETA(3,I)*OC(IJ,J,K)*ANM(3,M,L)}
        CEF(K,J,L)=SIGN(L)*CEF(J,K,L)
899 CONTINUE
901 CONTINUE
    WRITE(6,1002) (P(2,I), I=1,15)
1002 FORMAT(32H1  VALUES OF CEF PARAMETERS USED/ 8H  A20R2=F10.3,7H A22
1R2=F10.3,7H B22R2=F10.3,7H A40R4=F10.3,7H A42R4=F10.3/8H  B42R4=
1 F10
2.3,7H A44R4=F10.3,7H B44R4=F10.3,7H A60R6=F10.3,7H A62R6=F10.3/
38H  B62R6=F10.3,7H A64R6=F10.3,7H B64R6=F10.3,7H A66R6=F10.3,
47H B66R6=F10.3)
    RETURN
    END
```

```

C   T H E O R Y 6 .....
C   THIS SUBROUTINE DIAGONALIZES CEF MATRIX PROVIDED BY CEFMAT AND
C   CALCULATES(DELTA E)T, THE TEMPERATURE DEPENDENT QUAD SPLITTING
C   IN TERMS OF SHIELDING PARAMETERS.
C       INPUT DATA
C       NPOINT=NO. OF POINTS THAT ARE TO BE CALCULATED FOR PLOTTING
C       IF NPOINT IS GREATER THAN OR EQUAL TO 150 THE TEMPERATURE
C       DEPENDENT QUAD SPLITTING IS ALSO PLOTTED ON THE MOSELY
C       PLOTTER
C       SCALE=SCALE FACTOR FOR TEMPERATURE SCALE
C       C20,C22=CEF PARAMETERS
C       DD=LABEL FOR PLOTS
C       YMIN,YMAX=MIN. AND MAX. VALUES OF QUAD SCALE IN CM/SEC
SUBROUTINE THEORY(IQ,JQ,KQ,IOP)
COMMON GIVE,S,E,R,V,P,X,QSQ,NE,NP,IQ,JQ,KQ,IOP,XTEST,NFORM,NMOVE,A
COMMON/COMDER/DR(300),DS(300)
COMMON/COMHER/EVENUP,W(13),H(78),SPARE(79)
COMMON/COMTH/CEF(13,13,2)
DIMENSION QZZ(13),QXY(13),DD(10),C(13,13),EX(13,100)
DIMENSION GIVE(300)
DIMENSION E(100),R(100),V(100),P(3,20),X(20),QSQ(3),DP(20),S(1500)
DIMENSION EVECI(13),EVECR(13)
COMPLEX H,C,CTEMP,CMLPX
COMPLEX CSQRT, CONJG, CABS
IF(NFORM)1,2,1
2 CALL CEFMAT(1,2,2)
DO 3 I=1,13
W(I)=CEF(I,1,1)
3 CONTINUE
I=1
DO 4 J=1,12
JP1=J+1
DO 4 K=JP1,13
H(I)=CMLPX(CEF(J,K,1),CEF(J,K,2))
I=I+1
4 CONTINUE
SPARE(79)=0.0
DELTA=1.0E-10
CALL HERM(H,13,C,0,DELTA,IT)
C   MULTIPLY C BY PROPER PHASE FACTOR
DO 1000 I=1,13
TEMP=REAL(C(I,7))
IF(TEMP.NE.0.0) GO TO 1001
CTEMP=CSQRT(-CONJG(C(I,12))/C(I,2))
GO TO 1002
1001 CTEMP=CONJG(C(I,7))/CABS(C(I,7))
1002 DO 1003 J=1,13
1003 C(I,J)=CTEMP*C(I,J)
1000 CONTINUE
C   REARRANGE ENERGIES AND WAVE FUNCTIONS
DO 5 I=1,12

```

```

IP1=I+1
DO 5 J=IP1,13
IF(W(I)-W(J))5,5,7
7 TEMP=W(I)
W(I)=W(J)
W(J)=TEMP
DO 8 K=1,13
CTEMP=C(I,K)
C(I,K)=C(J,K)
8 C(J,K)=CTEMP
5 CONTINUE
C RENORMALIZE THE ENERGIES
TEMP=W(1)
DO 9 I=1,13
9 W(I)=W(I)-TEMP
C CALCULATE MATRIX ELEMENTS OF  $3J_z^2 - J(J+1)$  AND  $3/2(J^2 + J_m^2)$ 
DO 10 I=1,13
QZZ(I)=0.0
DO 10 J=1,13
QZZ(I)=QZZ(I)+REAL(CONJG(C(I,J))*C(I,J))*(3.0*(FLOAT(J)-7.0)
1 **2-42.0)
10 CONTINUE
DO 11 I=1,13
QXY(I)=0.0
DO 11 J=3,13
AJ=J-7
QXY(I)=QXY(I)+1.5*REAL(CONJG(C(I,J))*C(I,J-2)+C(I,J)*
1 CONJG(C(I,J-2)))*SQRT((6.0+AJ)*(5.0+AJ)*(7.0-AJ)*(8.0-AJ))
11 CONTINUE
READ(5,100) NPOINT,SCALE,C20,C22
100 FORMAT(I4,F10.5/2F20.5)
B=0.695056
E2Q=0.769854
HCE=0.8610308E-5
R2=0.19
R3=75.5
ALPHA=1.0196651E-02
C CALCULATE THE PARTITION FUNCTION
1 IF(IOP)12,13,12
13 M1=NPOINT
GO TO 15
12 M1=NE
IF(NFORM)15,14,15
14 DO 19 M=1,M1
16 T=V(M)
18 DO 19 N=1,13
EX(N,M)=EXP(-W(N)/(B*T))
19 CONTINUE
DIR1=0.5*E2Q*4.0*HCE*C20/R2*(-1.0)
DIR2=0.5*E2Q*4.0*HCE*C22/R2*(-1.0)
C4F=0.5*E2Q*ALPHA*R3*(-1.0)

```

```

15 CONTINUE
C   FEED IN THE PARAMETERS AND CALCULATE THE QUAD SPLITTING
    GAMMAR=P(KQ,1)
    GAMMAS=P(KQ,2)
    GO TO (50,51),IQ
50  GAMMAR=P(JQ,1)
    GO TO 52
51  GAMMAS=P(JQ,2)
52  CONTINUE
    DO 20 J=1,M1
      IF(IOP)70,71,70
71  T=SCALE*FLOAT(J)
    DO 72 I=1,13
72  EX(I,1)=EXP(-W(I)/(B*T))
      JAP=1
70  IF(IOP.NE.0) JAP=J
      PART=0.0
      DO 21 I=1,13
21  PART=PART+EX(I,JAP)
      QZZA=0.0
      QXYA=0.0
      DO 22 I=1,13
22  QZZA=QZZA+QZZ(I)*EX(I,JAP)
      QXYA=QXYA+QXY(I)*EX(I,JAP)
      SA=C4F*QZZA/PART
      SAA=SA*(1.0-GAMMAR)+DIR1*GAMMAS
      IF(DIR2)2001,2000,2001
2000 S(J)=SAA
      GO TO 2002
2001 SB=C4F*QXYA/PART
      SBB=SB*(1.0-GAMMAR)+DIR2*GAMMAS
      S(J)=SQRT(SAA**2+1.0/3.0*SBB**2)
2002 IF(IOP)23,20,23
23  CONTINUE
      DR(J)=- (SAA*SA+SBB*SB/3.0)/S
      DS(J)=(SAA*DIR1+SBB*DIR2/3.0)/S
20  CONTINUE
      IF(IOP)24,25,24
25  WRITE(6,200) IT
200  FORMAT(32H  NUMBER OF ITERATIONS IN HERM = 15 /
1      48H0  ENERGY          MIXING COEFFICIENTS/
2117H  (CM-1)  MJ=      -6      -5      -4      -3      -2      -1
3      0      +1      +2      +3      +4      +5      +6// )
      DO 30 I=1,13
      DO 31 J=1,13
      EVECR(J)=REAL(C(I,J))
31  EVECI(J)=AIMAG(C(I,J))
      WRITE(6,201)W(I),(EVECR(J), J=1,13),(EVECI(K), K=1,13)
201  FORMAT(F10.3,6X 13F8.3/16X 13F8.3)
30  CONTINUE
      WRITE(6,202)QZZ,QXY

```

-117-

```
202 FORMAT(18H0 (3JZ**2-J(J+1))//6E20.8/6E20.8/E20.8/22H0 1.5*(J+**2
1 + J-**2)//(6E20.8))
      READ(5,203) DD,YMIN,YMAX
203 FORMAT(10A6/2F20.5)
      WRITE(6,204) DD,SCALE,(S(I),I=1,M1)
204 FORMAT(22H1 RESULTS OF PLOT OF 10A6/10X 15H SCALE FACTOR=
1 F10.2//(2X 20F6.3))
      IF(NPOINT.LT.150) GO TO 32
      CALL CPLOT(S,M1,M1,DD,YMAX,YMIN,1)
32 CALL JPLOT(S,M1,120,YMIN,YMAX,SCALE,0.0,DD,1)
24 RETURN
      END
```

HITEMP

The required card decks are:

1. THEORY 5
 2. DERIV 2
 3. SEARCH
 4. QSQUAR
 5. OUTPUT
 6. COREL
 7. JPLOT
- see listings for QTAVE

The listings of decks 1-2 follow.

```

C      T H E O R Y   5 . . .
C      THIS SUBROUTINE CALCULATES THE QUADRUPOLE SPLITTING IN THE FORM
C      OF A/T+B
C      INPUT DATA
C      TEMP=INITIAL TEMPERATURE WHERE PLOT IS TO START
C      SCALE=MAX. TEMPERATURE/40
C      DD=LABEL FOR PLOT
SUBROUTINE THEORY(IQ,JQ,KQ,IOP)
COMMON GIVE,S,E,R,V,P,X,QQSQ,NE,NP,IQ,JQ,KQ,IOP,XTEST,NFORM,NMOVE,A
COMMON/COMDER/S4F,SLAT
DIMENSION GIVE(300),S4F(120)
DIMENSION DD(10)
DIMENSION E(100),R(100),V(100),P(3,20),X(20),QQSQ(3),DP(20),S(300)
IF(NFORM)1,1,2
1  R2=0.19
   R3=74.0
   ALPHA=1.0201E-2
   ALPHA2=ALPHA*ALPHA
   J=6
   SUM=J*(J+1)*(2*J+1)*(2*J-1)*(2*J+3)/5
   RM1=1.0
   B=0.695056
   E2Q=0.769854
   HCE=0.8610308E-5
   ANUM=-0.5*E2Q*R2*R3*ALPHA2*SUN*RM1/(13.0*B)
   ALAT=0.5*E2Q*HCE*4.0
   READ(5,100)TEMP,SCALE
100 FORMAT(2F20.5)
2  ANM=P(KQ,1)
   GAMMA=P(KQ,2)
   GO TO (3,4),IQ
3  ANM=P(JQ,1)
   GO TO 5
4  GAMMA=P(JQ,2)
5  SLAT=-ALAT
   IF(IOP)6,7,8
7  M1=41
   GO TO 9
8  M1=NE
   GO TO 9
6  M1=1
9  DO 10 M=1,M1
   IF(IOP)11,12,13
11 T=V(NE)
   GO TO 14
12 T=TEMP+SCALE*FLOAT(M)
   GO TO 14
13 T=V(M)
14 S4F(M)=-ANM/T
   S(M)=-ANM*S4F(M)-GAMMA*SLAT
10 CONTINUE

```

```
      IF(IOP)15,16,15
16  P(2,2)=P(2,2)/P(2,1)
      WRITE(6,200) P(2,1),P(2,2)
200  FORMAT(28H0  SQRT(A20**2 + 1/3A22**2)=  F10.2,22H  (1-GAMMA)/(1-SI
      1GMA)=  F10.2)
      READ(5,101)DD
101  FORMAT(10A6)
      WRITE(6,102)DD,TEMP,SCALE
102  FORMAT(50H1  PLOT OF TEMPERATURE VS QUADRUPOLE SPLITTING IN 10A6/
      140H0  NO. OF POINTS = 41      INITIAL TEMP = F10.1,
      218H  SCALE FACTOR =  F10.1)
      WRITE(6,103)(S(I), I=1,M1)
103  FORMAT(2X  20F6.3)
      CALL JPLOT(S,41,41,0.0,10.0,SCALE,TEMP,DD,1)
15  RETURN
      END
```

```
C      DERIV 2...
C      THIS FUNCTION CALCULATES THE PARTIAL DERIVATIVE OF THE OUTPUT
C      OF THE SUBROUTINE THEORY WITH RESPECT TO THE PARAMETER IP AT THE
C      POINT JP.
C      DERIV2 IS FOR THE SPECIAL CASE OF THE SHIELDING PARAMETERS
C      ONLY.
      FUNCTION DERIV(IP,JP)
      DIMENSION E(100),R(100),V(100),P(3,20),X(20),QSQ(3),S(300)
      DIMENSION GIVE(300)
      DIMENSION S4F(120)
      COMMON GIVE,S,E,R,V,P,X,QSQ,NE,NP,IQ,JQ,KQ,IOP,XTEST,NFORM,NMOVE
      COMMON/COMDER/S4F,SLAT
      CALL THEORY(1,2,2,1)
      IF(IP-1)10,10,20
10  DERIV=-S4F(JP)
      GO TO 30
20  DERIV=-SLAT
30  RETURN
      END
```